RSC Advances

ROYAL SOCIETY OF CHEMISTRY

www.rsc.org/advances

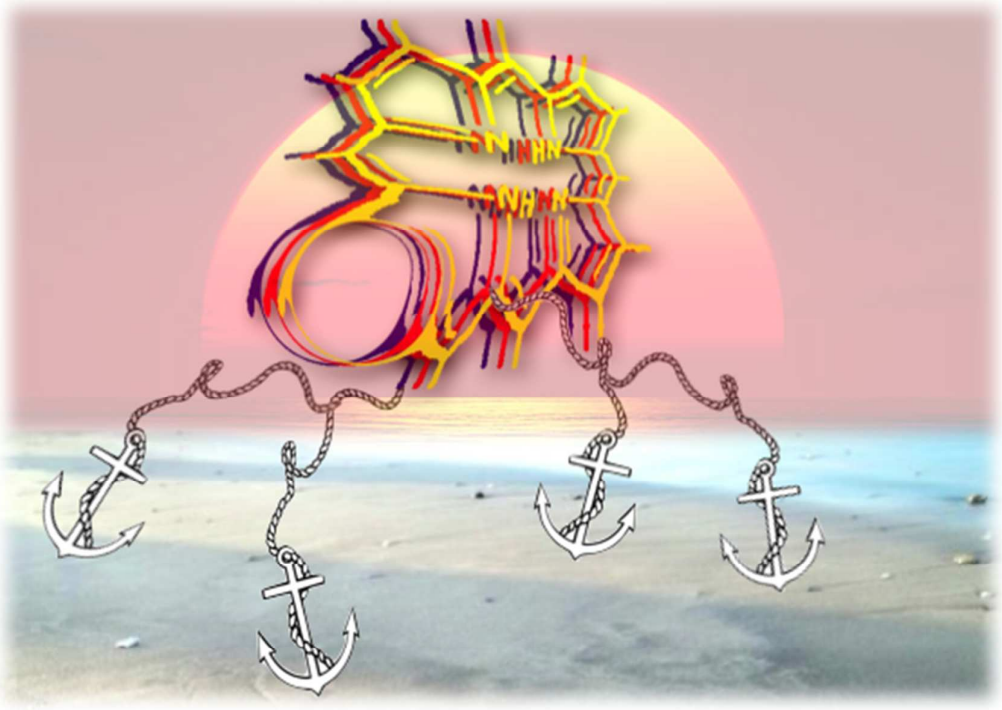

The influence of different anchoring groups in the efficiency of porphyrin dye sensitized solar cells.

RSC Advances review

The importance of various anchoring groups attached on porphyrins as potential dyes for DSSC applications.

K. Ladomenou, [§] **T. N. Kitsopoulos,** [¶] **G. D. Sharma*** [†], **A. G. Coutsolelos*** [§]

[§] Department of Chemistry, University of Crete, Laboratory of Bioinorganic Chemistry, Voutes Campus, P.O. Box 2208, 71003 Heraklion, Crete, Greece

[¶]Department of Chemistry UoC and IESL-FORTH, P.O Box 1527, 71110 Heraklion, Crete

[†] R&D Centre for Engineering and Science, JEC Group of Colleges, Jaipur Engineering College Campus, Kukas, Jaipur, Raj 303101, India

Corresponding AuthorsE-mail: coutsole@chemistry.uoc.gr (A.G.C.); gdsharma273@gmail.com (G.D.S.).

TABLE OF CONTENTS

ABSTRACT

In the design of new chromophores, with high efficiency, chemical stability and low cost materials for dye sensitized solar cells, porphyrin macrocycles could play a very important role. Their successful use in nature during photosynthesis must be the inspiration for new artificial antenna systems. Porphyrins offer an excellent platform for building such multi-chromophoric systems to self-assembly because of the availability of several substituent sites and their intrinsic spectroscopic properties. Specifically, their high absorption ability in the visible region can be extended, electron donor and anchoring groups with high chemical affinity onto the cell, should be part of the new design.

This review provides a summary of some of the most important developments and approaches that are used in order to improve the light collection efficiency of DSSCs based on porphyrin hybrid derivatives. For this reason we have attempted to describe the developments in the DSSCs of various porphyrin dyes with different anchoring groups linked through either *meso* or *β*-positions. Also, the influence of the anchoring

groups in the cell performance is discussed. Studies containing chromophores other than porphyrin derivatives are not included in this work.

1. INTRODUCTION

The increasing demand for energy and the continuous depletion of fossil fuels creates an urgent need to discover alternative energy supplies. Hence, further research to explore alternative, safe and renewable sources of energy is extremely important. Among all renewable energy technologies, photovoltaics, which utilize solar energy, are believed to be the most promising ones. Solar energy, one of the most abundant and renewable sources of energy, plays an important role, as the amount of energy emitted from the sun to earth is several thousand times higher than the global requirement. At present most of the solar cells are fabricated from silicon. However, this type of solar cells has certain limitations due to the difficulties related to large scale production and high fabrication cost.

Since their first report of Grätzel research group in 1991, [1,2] dye sensitized solar cells (DSSCs) have attracted lots of attention globally because of their low cost and environmentally friendly properties. These solar cells have the potential to replace the present conventional solar cells based on silicon. [3-5] The operation of the typical solar cell is illustrated in Figure 1, which consists of a dye sensitized mesoporous working electrode (generally wide energy band gap metal oxide semiconductor TiO_2 or ZnO anode), a counter electrode (Pt coated cathode) and an electrolyte (iodide based or cobalt complex, redox mediator), filling the space between the anode and cathode. When the DSSC is illuminated, electrons of the sensitizer are excited to the lowest unoccupied molecular orbital (LUMO), then are rapidly injected into the conduction band of metal oxide semiconductor (TiO_2), and subsequently transferred to the platinized counter electrode through the external circuit. The holes are reduced by the redox couple, either I_3^- / I^- or Co^{2+} / Co^{3+}, and the oxidized dye thereby regenerated by the I^- spices or Co^{2+} complex to produce I_3^- spices or a Co^{3+} complex. Finally, the diffusion of oxidized spices i.e. I_3^- or a Co^{3+} complex, to the surface of the cathode complete the circuit.

A plethora of photophysical sequences occur in a DSSC, all of which are dependent on the three main components of the DSSC: the light absorber (dye), the electron transport agent (wide band gap nanocrystalline semiconductor, mostly TiO_2 or ZnO), a hole transport agent (redox couple in electrolyte). For an efficient DSSC, all three components require fine tuning.[6] In particular, concerning the dye, there are certain features required for efficient performance such as suitable HOMO and LUMO levels for charge injection into TiO_2, dye regeneration from electrolyte, an anchoring group to attach to the semiconducting material, and a broad absorption in the visible and NIR region for light harvesting, as well as photostability and solubility.[7]

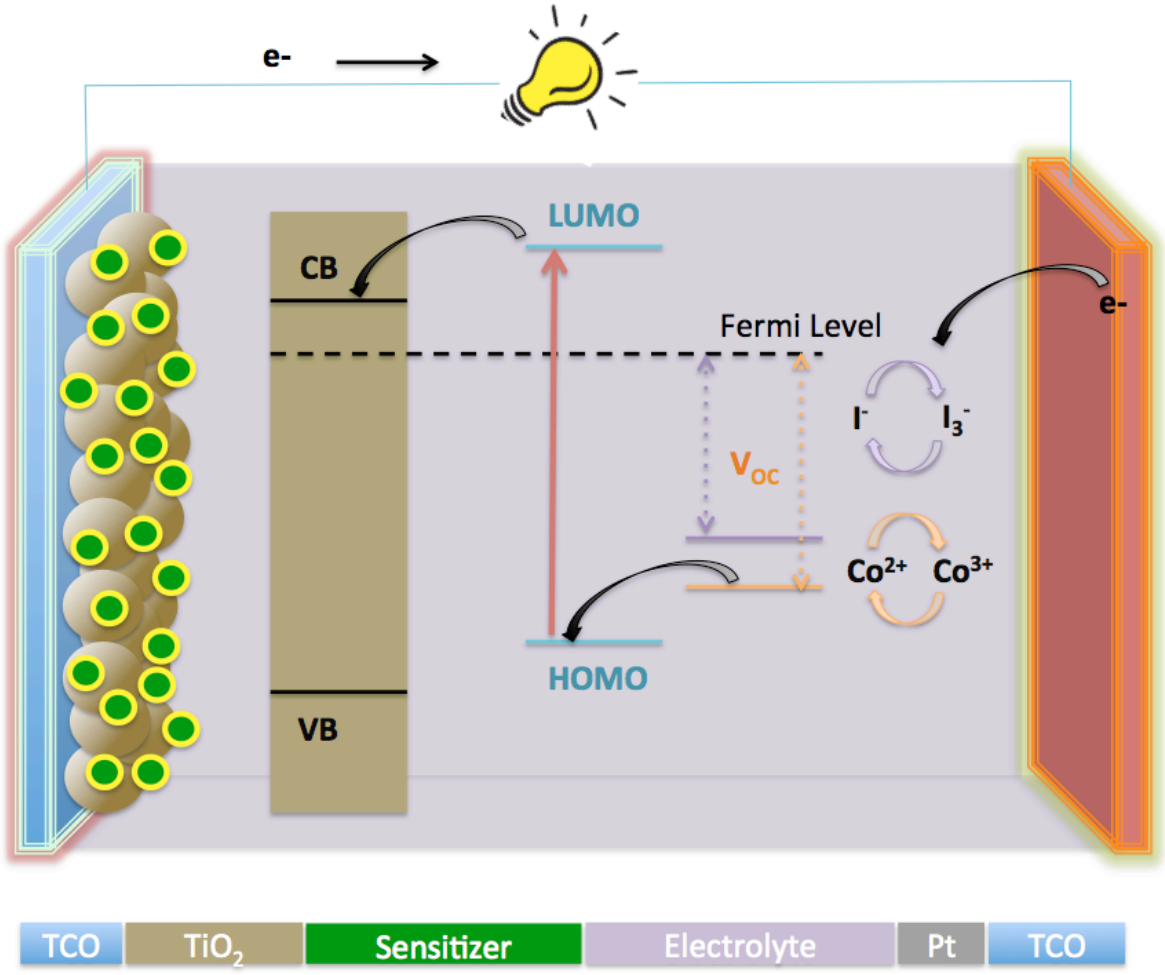

Figure 1. Systematic illustration of components and operation of dye sensitized solar cell

The DSSCs based on nanocrystalline TiO_2 photoanode sensitized with polypyridyl ruthenium complexes have yielded power conversion efficiency (PCE) over 11%.[8-13] However, high cost, scarcity and environmental issues concerning the

ruthenium complex limits their affordable commercial applications, and has prompted the exploration of lower cost and safer sensitizers. Consequently, scientists from all over the world have put a significant amount of effort into the design of new efficient DSSCs, using either no-metal -or inexpensive-metals, and sensitizers, with high molar extinction coefficients.[5,14-20] Moreover, this new DSSCs, are prepared using facile synthesis, flexible structural modification and ideal photovoltaic performances. The PCE's of the DSSCs sensitized with metal free dyes were reported to be 9-10 % during last five years. The best performing DSSC sensitizer is one with an organic dye (C219) that achieved a PCE of 10.3 %.[21] This value however, remains lower than the state of the art ruthenium complex dyes, because of its weak light absorption in the near infrared region.

Therefore, it is significant to develop efficient sensitizers over a very wide spectral range for DSSCs. Inspired by the efficient energy and electron transfer behavior in the light harvesting antenna of natural systems,[22] porphyrin derivatives[23,24] and analogues[25,26] have been widely used in photovoltaic devices. Porphyrin based compounds have several intrinsic advantages such as good photostability and rigid molecular structure with large absorption coefficients in visible region.[16,27,28] Their photophysical and electrochemical properties can be tuned by peripheral substituents and inner metal complexations, by taking advantage of their multiple reactive sites, including four *meso* and eight *β*-positions, [29-35] A drawback of porphyrins is the poor light-harvesting properties at wavelengths around 450 nm and above 600 nm. Elongation of strong electron-donating and electron-withdrawing groups can shift and broad the absorption of porphyrins making it possible to increase the light-harvesting property and the resulting DSSC efficiency. Therefore, a push-pull type porphyrin dye with diarylamine (donor) and ethynyl-benzoic acid (acceptor) substituents at *meso* positions has been reported to achieve a PCE of 12.3%,[36] which remains the highest value for DSSCs so far and superior than Ru based DSSCs. This encouraging achievement stimulates the development of further porphyrin sensitizers to promote the performance of the DSSCs.

In DSSCs the presence of an anchoring group is essential to graft the dye on a TiO_2 surface, in order to achieve fast electron injection into the TiO_2 semiconductor.[37] The efficiency of the electron-transfer step at the dye-semiconductor interface is highly dependent, among numerous other factors, on the way the chromophore is attached to

the surface.[38-40] Therefore, different porphyrin anchoring groups have been used and researchers have studied their effect on the TiO_2 surface.[41-43]

This review provides a summary of some of the most important developments and approaches that were used in order to improve the light collection efficiency of DSSCs based on porphyrin hybrid derivatives. Studies concerning various synthetic approaches of porphyrins are not described. This manuscript is mainly focused on the influence of the various anchoring groups used for the attachment of the porphyrin derivatives to the TiO_2 electrode.

2. CARBOXYLIC ACIDS AS ANCHORING GROUPS

Carboxylic acid present in the *meso* and *β*–positions of a porphyrin ring is an anchoring group that has been extensively studied. At the *meso*-position, two main classes of linking moieties have been employed most often, the classic *meso*-substituted benzoic acid linking and the direct attachment of a *meso*-alkynylbenzoic acid moiety. For DSSCs employing a *β*–position linking group the conjugated ones have been mostly studied in the literature.

Carboxylic acid groups can form ester linkages with the surface of the metal oxide to provide a strongly bound dye and good electronic communication between the two parts. However, the link can be hydrolyzed through the presence of water, an important factor in terms of the stability of the cell. For carboxylate groups, bidentate connections have been shown to be the preferred binding mode on TiO_2.[44-46]

2.1 *Meso*-Substituted Benzoic Acids

The concept for the design of *meso* ethynyl linked porphyrins was first given by Anderson[47] and Therien.[48] Before the discovery of DSSC, the ability of porphyrin to sensitize TiO_2 semiconductor was first demonstrated by Grätzel in 1987.[49] However, Kay and Grätzel first introduced a porphyrin as a sensitizer in DSSC in 1993. A substituted porphyrin with propionic acid as anchoring group achieved an overall efficiency of 2.6% (J_{sc} = 9.4 mA/cm^2, V_{oc} = 0.52 V).[50]

Cherian and Wamser[51] in 2000 reported the first *meso*-substituted DSSC with 3.5% (J_{sc} = 0.133 mA/cm^2, V_{oc} = 0.36 V, and *FF* = 0.62) efficiency based on a free-base porphyrin **1** (Figure 2). That report also analyzed the adsorption properties of **1** on TiO_2 using XPS and resonance Raman spectroscopy to elucidate the binding characteristics of **1** and reported that low concentrations of dye in the adsorption solution (~0.1 mM) are important to avoid dye aggregation.

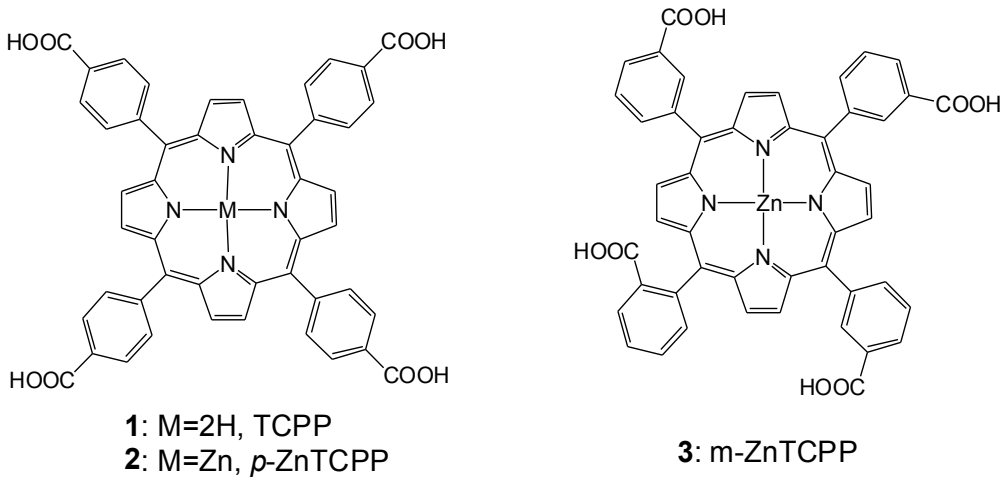

Figure 2. Molecular structures of porphyrins **1, 2** and **3**

One key issue to consider in designing porphyrin dyes relates to the position of the anchoring group in relation to the plane of macrocycle π-system. The presence of carboxyl anchoring groups attached to the *meso*-phenyl ring of the porphyrin has little influence on the ground-state electronic nature of the dye, because of the orthogonal orientation of the *meso*-phenyl ring.[52-54] However, a few studies have shown that the positioning of carboxyl group vary the performance of the solar cells.[42,51,55-57] For example, Campbell *et al.* have reported a 5-fold increase in the short circuit photocurrent (J_{sc}) and a significantly higher open circuit photovoltage (V_{oc}) on changing the position of the COOH groups from the *para* (in *p*-ZnTCPP **2**) to the *meta* position (in *m*-ZnTCPP **3**) (Figure 2).[15] This effect was attributed to a more efficient electron injection from the *meta* porphyrin, which binds flat on the TiO_2 surface, compared to that of the *para*, which binds vertically (Figure 3).[15]

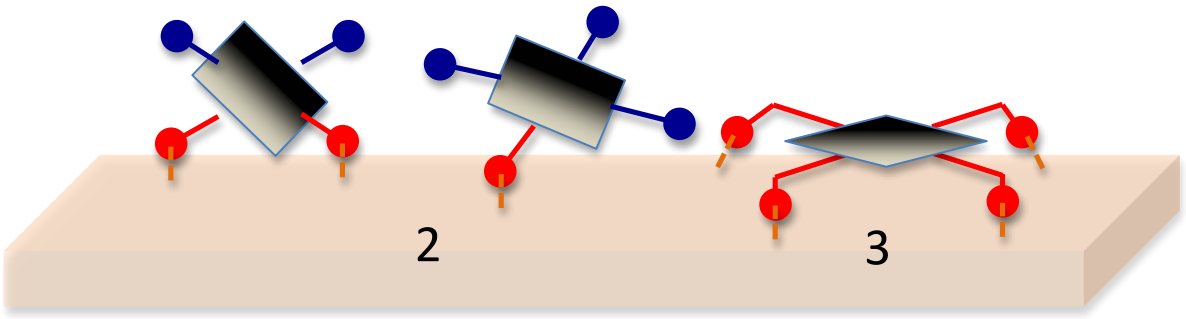

Figure 3. Different binding modes of porphyrins **2** and **3** onto TiO_2 surface.

In 2007 Galoppini and coworkers[55] studied tetrachelated zinc porphyrins with four *meta*-substituted linkers at four *meso* positions of the porphyrin to give inside on how the distance and attachment of the sensitizing chromophore on colloidal TiO_2 and ZnO films influence interfacial processes and solar cell efficiencies. The *meta* substitution favored a planar binding mode to the metal oxide surfaces, as determined by a combination of studies that included IR, UV, and solar cell efficiencies on TiO_2. All studies indicated that only *p*-ZnTCPP **2** aggregated, suggesting close packing of the dye molecules on the semiconductor surface. Aggregation effects were not observed for the *meta* porphyrins. The greater efficiency of the rigid planar *meta*-substituted systems was explained in terms of a greater charge injection into the TiO_2 semiconductor from rings that lie flat, and closer, to the surface.In the same study it was observed that the main binding modes for this class of molecules are a chelating and/or a bidentate bridging of the carboxylate on the TiO_2 surface (Figure 4).[45,58-60]

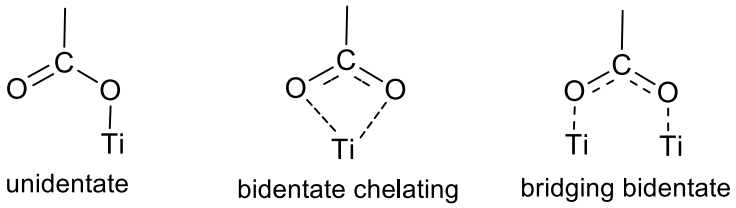

Figure 4. Main binding modes of the carboxylate group to TiO_2.

In 2009, Imahori *et al.* studied a series of monocarboxyphenyl triaryl porphyrins in DSSCs.[61] Zn porphyrin **4** (Figure 5) yielded the highest efficiency of 4.6% (J_{sc} = 9.4 mA/cm^2, V_{oc} = 0.76 V, and *FF* = 0.64) in a standard DSSC. As a part of their study, they

optimized the adsorption time and adsorption solvent for dye loading on TiO_2 films and determined that lower adsorption times and protic solvents (methanol) led to the best efficiencies. In an another publication from the same group integration of a push-pull structure with a *trans* diphenylamino substituent **5** gave a very high efficiency of 6.5% (J_{sc} = 13.1 mA/cm^2, V_{oc} = 0.72 V, and *FF* = 0.69) (Figure 5).[62]

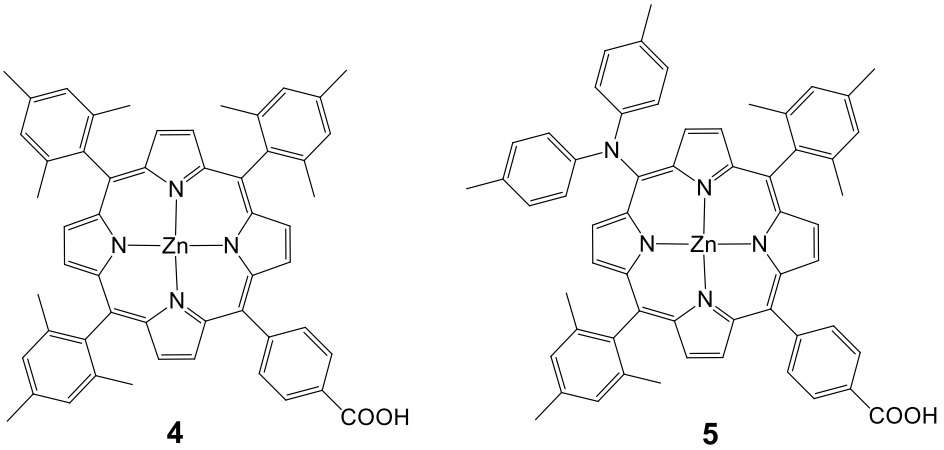

Figure 5. Molecular structures of porphyrins **4, 5**

Moreover, in order to synthesize a dye with a broad spectral coverage two porphyrin units can be linked at the *meso* position either directly[63] or by suitable π-conjugated linker.[64] Furthermore, unsymmetrical porphyrin dyads can lead to enhancement of the solar cell efficiency.[65] Combining the strategy of donor substation and the "built-in" energy gradient of the hetero-dimer taking advantage of the different energy levels of zinc coordinated and non-coordinated porphyrins,[65] Segawa *et al*. synthesized a N-fused carbazole zinc porphyrin-free base porphyrin triad and obtained highly efficient light to current conversion throughout the visible to NIR region.[66] The same research group synthesized ethynyl-linked porphyrin hetero-dimers substituted by a series of electron donors, namely, 3,6-di-tert-butylphenyl **6**, bis(4-methoxyphenyl)amino **7**, bis (4-tert-butylphenyl)amino **8** and 3,6-di-tert-butylcarbazol-9-yl **9** (Figure 6).[58] Despite the increased electron injection driving forces due to the bathochromic shift, the intensification of long-wavelength absorption bands and the elevated LUMO levels, the substitution of diphenylamino groups (**7** and **8**) with stronger electron-donating abilities gave rise to surprising mediocrity in the short-circuit photocurrent densities (J_{sc}). For that reason the overall energy conversion efficiencies followed the order **7** (3.94%) (J_{sc} = 10.55 mA/cm^2, V_{oc} = 0.543 V, and *FF* = 0.69) < **6**

(4.57%) (J_{sc} = 12.51 mA/cm^2, V_{oc} = 0.541 V, *FF* = 0.68) < **8** (4.83%) (J_{sc} = 13.15 mA/cm^2, V_{oc} = 0.541 V, *FF* = 0.68) < **9** (5.21%) (J_{sc} = 14.26 mA/cm^2, V_{oc} = 0.547 V and *FF* = 0.67).

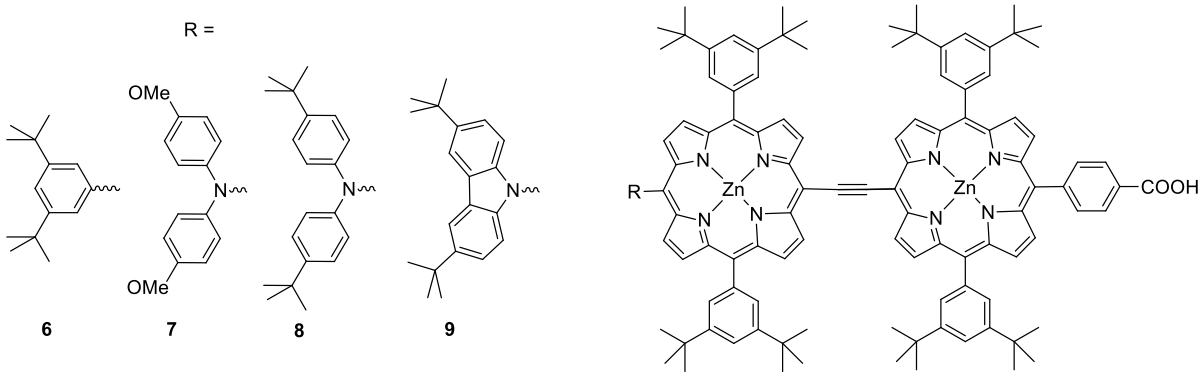

Figure 6. Molecular structures of the dyes studied **6-9**.

Table1: Photovoltaic performances of DSSCs using **6-9** as sensitizers.

Dye	V_{oc}, mV	J_{sc}, mA cm^{-2}	FF	*n*, %
6	541	12.5	0.68	4.6
7	543	10.5	0.69	3.9
8	541	13.1	0.68	4.8
9	547	14.3	0.67	5.2

In 2013 D'Souza and *coworkers*[67] studied, 13 porphyrins functionalized with a carboxylic acid anchoring group at the *para*, *meta*, or *ortho* positions of one of the phenyl rings of *meso*-tetra aryl porphyrin in addition to varying functional groups of the remaining *meso* positions of the porphyrin ring (Figure 7). It was found that porphyrins anchored to the mesoporous TiO_2 in the *para* and *meta* positions with respect to the porphyrin ring had improved photoelectrochemical properties compared to their *ortho* counterparts. This was supported by femtosecond transient absorption spectroscopy data collected on zinc-metalated porphyrin derivatives, showing a fast charge recombination time for the *ortho* derivative adsorbed electrode. Similarly, placing tolyl groups in the three remaining *meso* positions showed improved efficiency compared to

the long alkyl chain and ethylene oxide groups mentioned in this study. Additionally, the zinc porphyrin derivatives outperformed their free-base porphyrin counterparts.

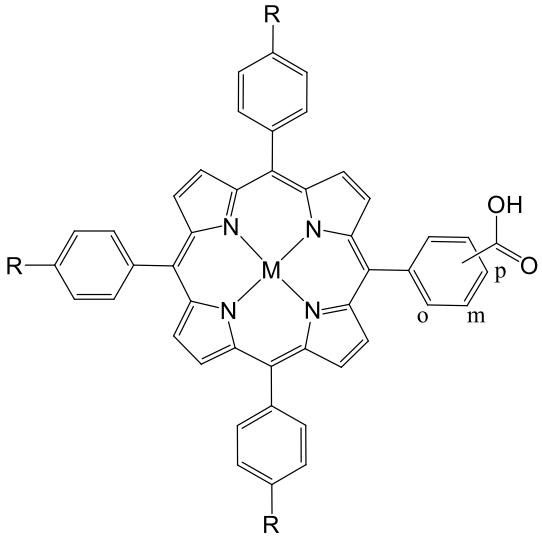

10: R=-CH_3; M=2H; para
11: R=-CH_3; M=2H; meta
12: R=-CH_3; M=2H; ortho
13: R=-CH_3; M=Zn; para
14: R=-CH_3; M=Zn; meta
15: R=-CH_3; M=Zn; ortho
16: R=-$(OCH_2CH_2)_3OCH_3$; M=2H; para
17: R=-$(OCH_2CH_2)_3OCH_3$; M=2H; meta
18: R=-$(OCH_2CH_2)_3OCH_3$; M=Zn; para
19: R=-$(OCH_2CH_2)_3OCH_3$; M=Zn; meta
20: R=-$CH_2CH_2CH_3$; M=2H; meta
21: R=-$CH_2CH_2CH_3$; M=Zn; para
22: R=-$CH_2CH_2CH_3$; M=Zn; meta

Figure 7. Molecular structures of dyes **10-22**.

1,3,5-triazine, a known mediator of intramolecular photoinduced electron transfer between chromophores, tethered two porphyrin units.[68] The synthesis was performed by taking advantage of the stepwise and temperature-dependent reactivity of cyanuric chloride. The dyads were also functionalized by a terminal carboxylic acid group of a glycine moiety attached to the triazine group (Figure 8). The study of the photophysical and electronic properties of the two compounds revealed no significant electronic interaction in their ground states but broadened spectral absorptions and suitable frontier orbital energy levels for use in DSSCs. Porphyrins **23** and **24** were fabricated for DSSC, demonstrating efficient intramolecular electron-transfer and charge-separation phenomena mediated by the triazine group. The PCE values were of 3.61% (J_{sc} = 8.82 mA/cm^2, V_{oc} = 0.63 V, and *FF* = 0.65) and 4.46% (J_{sc} = 9.94 mA/cm^2, V_{oc} = 0.66 V, and *FF* = 0.68), respectively. The higher PCE value of the **24**-based DSSC is attributed to its larger dye loading and higher J_{sc}, V_{oc}, and *FF* values.

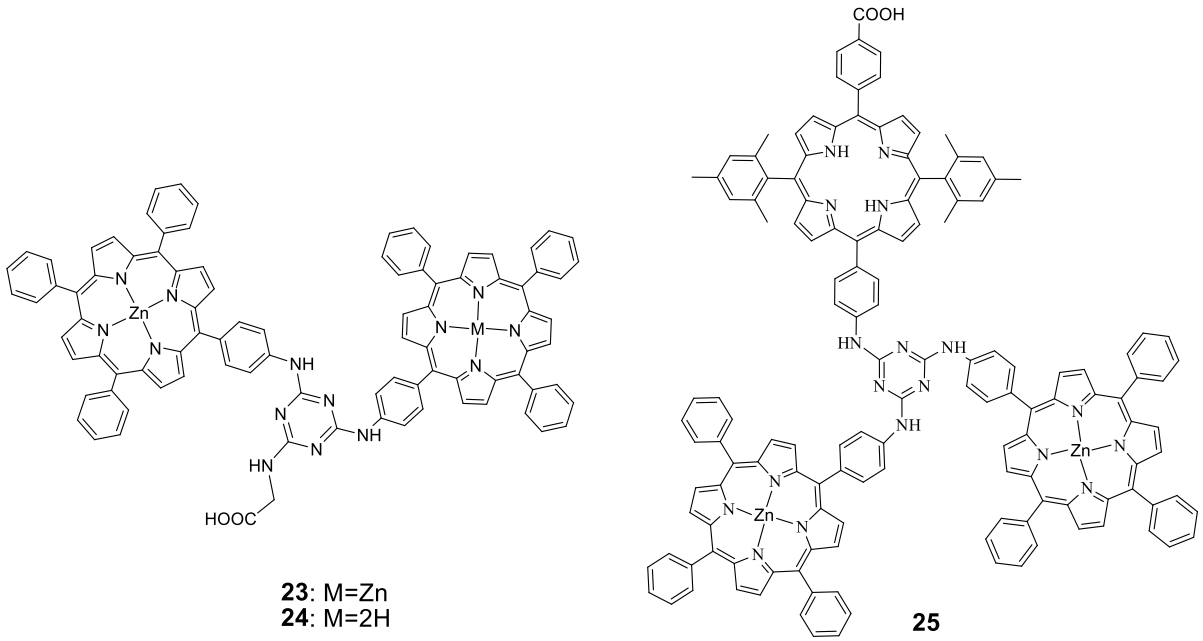

Figure 8. Molecular structures of porphyrins **23-25**

Coutsolelos and *coworkers*,[69] synthesized *via* stepwise amination reactions of cyanuric chloride a propeller shaped, triazine bridged, and unsymmetrical porphyrin triad **25**. Photophysical and electrochemical studies of the triad revealed no significant electronic interactions between the porphyrin units in the triad ground state, but the frontier orbital energy levels are suitable for use as sensitizer in DSSCs, as they favour the electron injection and dye regeneration processes. These results were corroborated by DFT calculations which suggested that the triad **25** could also be described as a "push-pull" 2D-π-A system, with the A residing on the anchoring (carboxylic acid) group, that has the potential to promote triazine-mediated electron transfer and injection into the TiO_2 electrode. Solar cells sensitized by triad **25** exhibited PCE of 4.91% (J_{sc} = 10.9 mA/cm^2, V_{oc} = 0.66 V, and *FF* = 0.68). The PCE of the latter solar cell was further improved up to 5.56% (J_{sc} = 12.4 mA/cm^2, V_{oc} = 0.64 V, and *FF* = 0.70) by co-sensitization by incorporation of chenodeoxychlolic acid (CDCA) in the dye solution (Table 2).

Table2: Photovoltaic performances of DSSCs using **23**-**25** as sensitizers.

Dye	V_{oc}, mV	J_{sc}, mA cm^{-2}	FF	n, %
23	630	8.8	0.65	3.6
24	660	9.9	0.68	4.5
25	660	10.9	0.68	4.9
25[a]	640	12.4	0.70	5.6

[a] co-sensitization with CDCA

Recently, Hung *et al.*[70] synthesized a series of porphyrins **26-31** (Figure 9) having two electron donating groups and dual anchoring units that were connected through a porphyrin π-bridging unit and applied as sensitizers for DSSCs. The highest PCE of about 4.07 % with J_{sc} = 9.81 mA/cm^2, V_{oc} = 0.63 V and *FF* = 0.66 was observed for **30** due to its high molar extinction coefficient (Table 3).

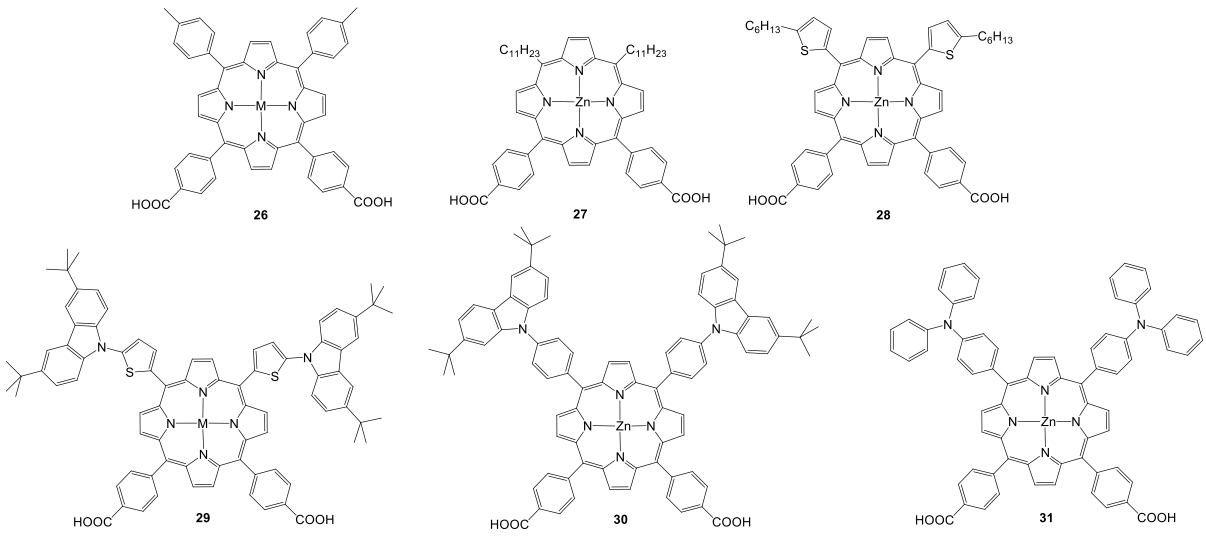

Figure 9. Molecular structures of **26-31**.

Table3: Photovoltaic performances of DSSCs using **26-31** as sensitizers.

Dye	V_{oc}, mV	J_{sc}, mA cm^{-2}	FF	n, %
26	570	7.52	0.65	2.78
27	580	8.50	0.58	2.85
28	580	7.92	0.69	3.18
29	580	6.87	0.68	2.72
30	630	9.81	0.66	4.07
31	590	9.18	0.67	3.64

Moreover, Hung *et al.* synthesized a series of 1D-π-3A zinc porphyrin dyes **32-36** with three *p*-carboxyphenyl anchoring groups with various substituents at the *meso* position (Figure 10).[71] Porphyrin **34** is slightly red shifted compared to the other porphyrins. The Soret band of **34**, **35**, **36** is broadened because of the presence of an electron donating amino unit. Higher than 5 % PCE has been achieved for a DSSC sensitized with either **34-36**. The strong electron donating character, better electron injection, intrinsic anti-aggregation and suppressed charge recombination capacity contributed to the highest PCE of 6.10 % (J_{sc}=12.66 mA/cm^2, V_{oc} =0.70 V and *FF* = 0.69) for the DSSC sensitized with **35** (Table 4). Moreover, it was demonstrated that the DSSC based on multi-anchoring unit porphyrin dye is more stable than their mono-anchoring analogs.

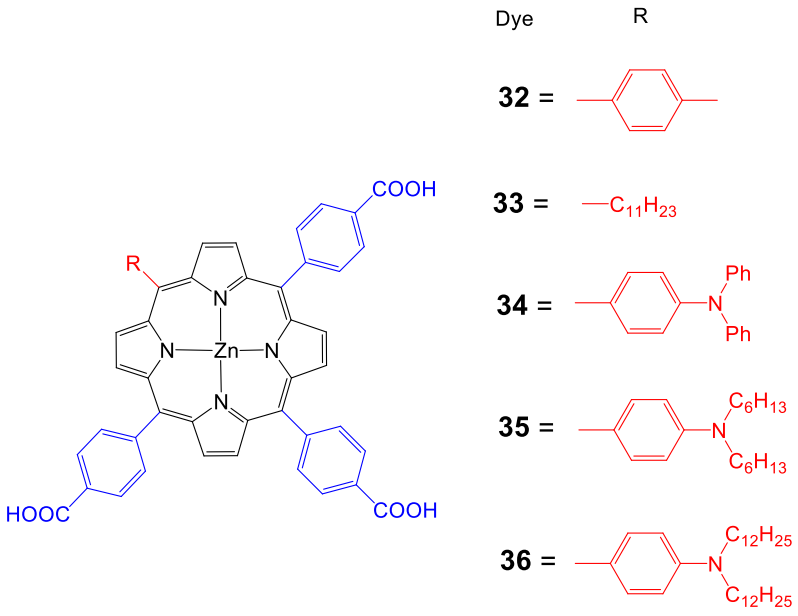

Figure 10. Molecular structures of dyes **32-36**.

Table 4: Photovoltaic performances of DSSCs using **32-36** as sensitizers.

Dye	V_{oc}, mV	J_{sc}, mA cm^{-2}	FF	n, %
32	630	10.55	0.68	4.51
33	590	9.36	0.69	3.80
34	660	11.75	0.69	5.36
35	700	12.66	0.69	6.10
36	650	13.61	0.66	5.80

Although *meso*-carboxyphenyl tethered porphyrins have been widely studied in DSSCs, there remains a concern about the torsional angle decoupling of the phenyl rings from the conjugated system of the macrocycle, which potentially limits the electronic communication between the excited dye and the linkage to the semiconductor. Therefore more attention has been paid to other structural designs such as porphyrins with *meso*-alkynylbenzoic acid or *β*-linked conjugated tethers and devices using these designs have reached remarkably high efficiencies.

2.2 Conjugated Bridge Carboxylic Acids

The type of linkage between the porphyrin and the binding group is very important. It has been shown that conjugated linkers make a significant difference in the overall cell performance.

2.2.1 *Meso*-Position Linking

The use of *meso*-linked alkynylbenzoic acid tethers is a relatively new design strategy in porphyrin DSSC research. The first report of alkynylbenzoic acid tethered porphyrins was by Stromberg *et al.* in 2007[72] in which the reported photocurrent of the device was only 0.035 mA cm^{-2}. Since then two main groups of Joseph Hupp and Eric Diau have studied this novel tether style. The use of the *meso*-alkynylbenzoic acid tether has led to an increase in solar cell efficiency for porphyrin DSSCs.[73,74] In a paper by Hupp and *coworkers*, dye **37** (Figure 11) was reported to give efficiencies of 2.5% (J_{sc}=5.9 mA/cm^2, V_{oc} =0.65 V and *FF* = 0.66) in standard TiO_2 DSSC.[75] In the report on **37**, ZnO was also tested as a semiconductor, and it was determined that the more acidic dyes that tend to slightly corrode the ZnO surface showed better electron injection dynamics.

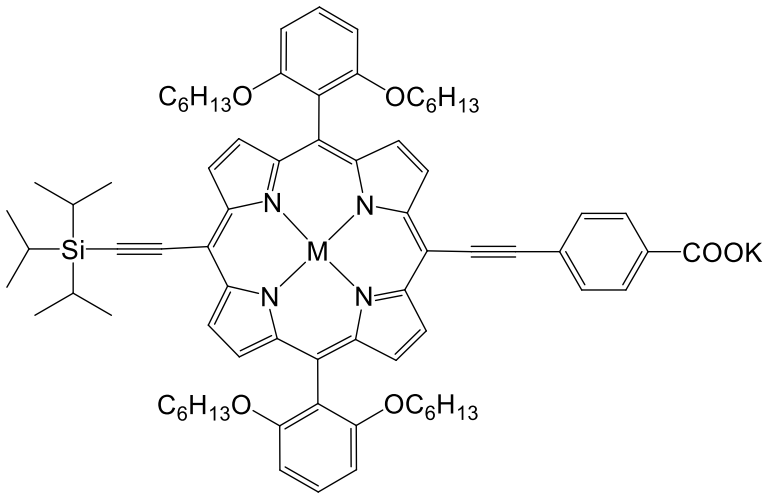

37

Figure 11. Molecular structure of compound **37**.

To solve the problem of porphyrin aggregation, 3,5-di-tertbutylphenyl groups were introduced at the *meso*-positions of the porphyrin ring. Based on this molecular design, Yeh and *coworkers*[35] reported *meso*-substituted zinc porphyrin derivatives, for

which **38** (Figure 12) served as a reference compound. With the diarylamino group attached at the *meso*-position of the porphyrin core, **39** attained 6.0% efficiency (J_{sc}=13.60 mA/cm^2, V_{oc} =0.701 V and *FF* = 0.629). The appearance of porphyrins with a push–pull framework such as **39** and **40** indicated the arrival of a new period of DSSC.[74] Porphyrin **40** had two long alkyl chains in order to improve the thermal and photochemical stability of a device with an efficiency of 6.8% (J_{sc}=13.68 mA/cm^2, V_{oc} =0.711 V and *FF* = 0.695), (Table 5).

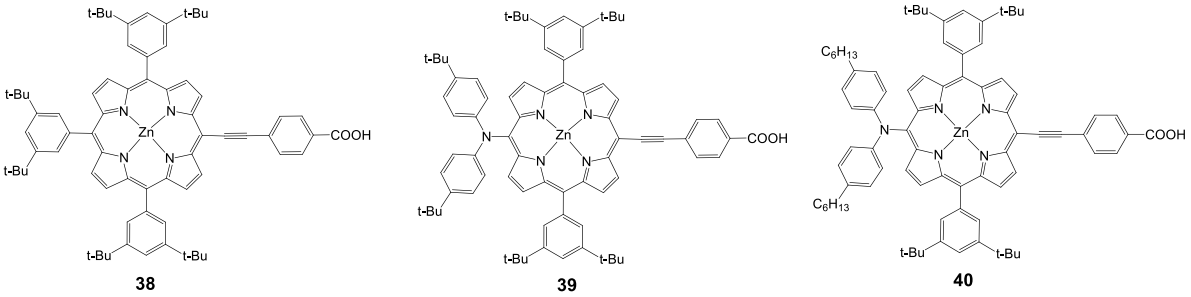

Figure 12. Molecular structures of dyes **38-40**.

Table5: Photovoltaic performances of DSSCs using **38**-**40** as sensitizers.

Dye	V_{oc}, mV	J_{sc}, mA cm^{-2}	FF	*n*, %
38	617	5.79	0.667	2.4
39	701	13.60	0.629	6.0
40	711	13.68	0.695	6.8

In 2010, the device performance of **40** was further improved by Grätzel and coworkers,[30] giving an efficiency of 10.9%, (J_{sc}=18.6 mA/cm^2, V_{oc} =0.77 V and *FF* = 0.76) which lasted as a record for DSSC until 2011. Diau and *coworkers* synthesized a series of dyes in order to probe the effects of the bridging moiety length and the size of the intermediate acene.[76-79] A series of porphyrin dyes with differing numbers of ethynylphenyl groups (1–4) were produced and tested; the optimal dye **41** (with n = 1) is shown in Figure 13 and gave an efficiency of 2.7% (J_{sc} = 7.3 mA/cm^2, V_{oc} = 0.57 V, and *FF* = 0.65).[77] In a different study in order to determine how the number of aromatic

rings in the bridging group affects solar cell performance, a series of porphyrin dyes with benzene through pentacene moieties were synthesized and tested as DSSCs. The optimal dye **42** is shown in Figure 13 and gave an efficiency of 5.4% (J_{sc} = 12.67 mA/cm^2, V_{oc} = 0.67 V, and *FF* = 0.64).[78]

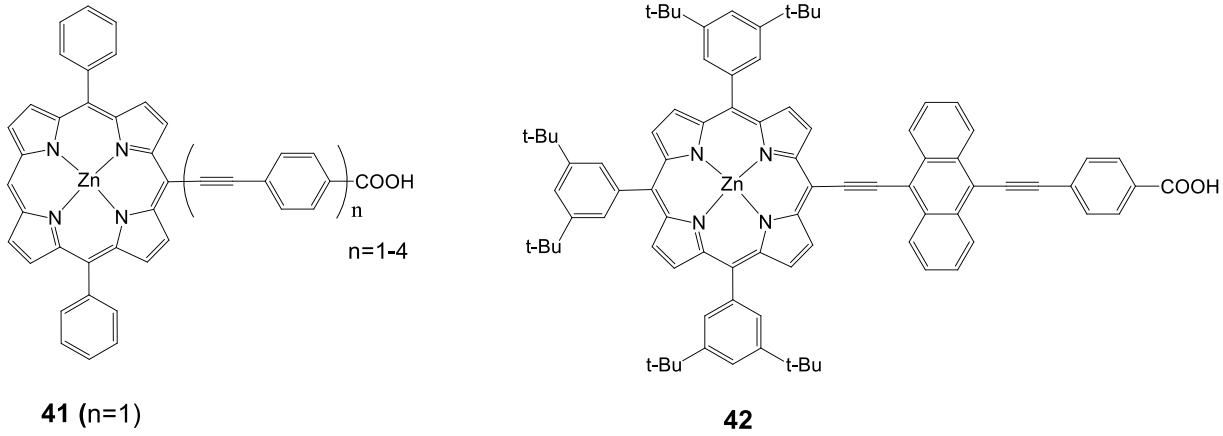

41 (n=1) **42**

Figure 13. Molecular structures of compounds **41** and **42**.

The electronic structure of porphyrins is considerably influenced by introducing electron donors at the *meso* positions.[29,30] In principle, the tuning of HOMO and LUMO levels could be achieved with the choice of suitable groups. Xie *et al.* synthesized porphyrins (**43-47**) with various number of triphenylamine and trimethoxyphenyl groups as electron donors, in order to modulate the HOMO and LUMO levels (Figure 14).[80] Among these porphyrin dyes, **47** showed the highest PCE of 5.45 % (J_{sc} = 15.36 mA/cm^2, V_{oc} = 0.665 V, and *FF* = 0.53), associated with an efficient electron injection and dye regeneration, resulting from the suitable arrangements of the HOMO and LUMO energy levels, in combination of longer electron lifetime. It was demonstrated that by introducing appropriate electron donors might significantly enhance the performance by modulating the HOMO and LUMO levels of the porphyrin sensitizers (Table 6).

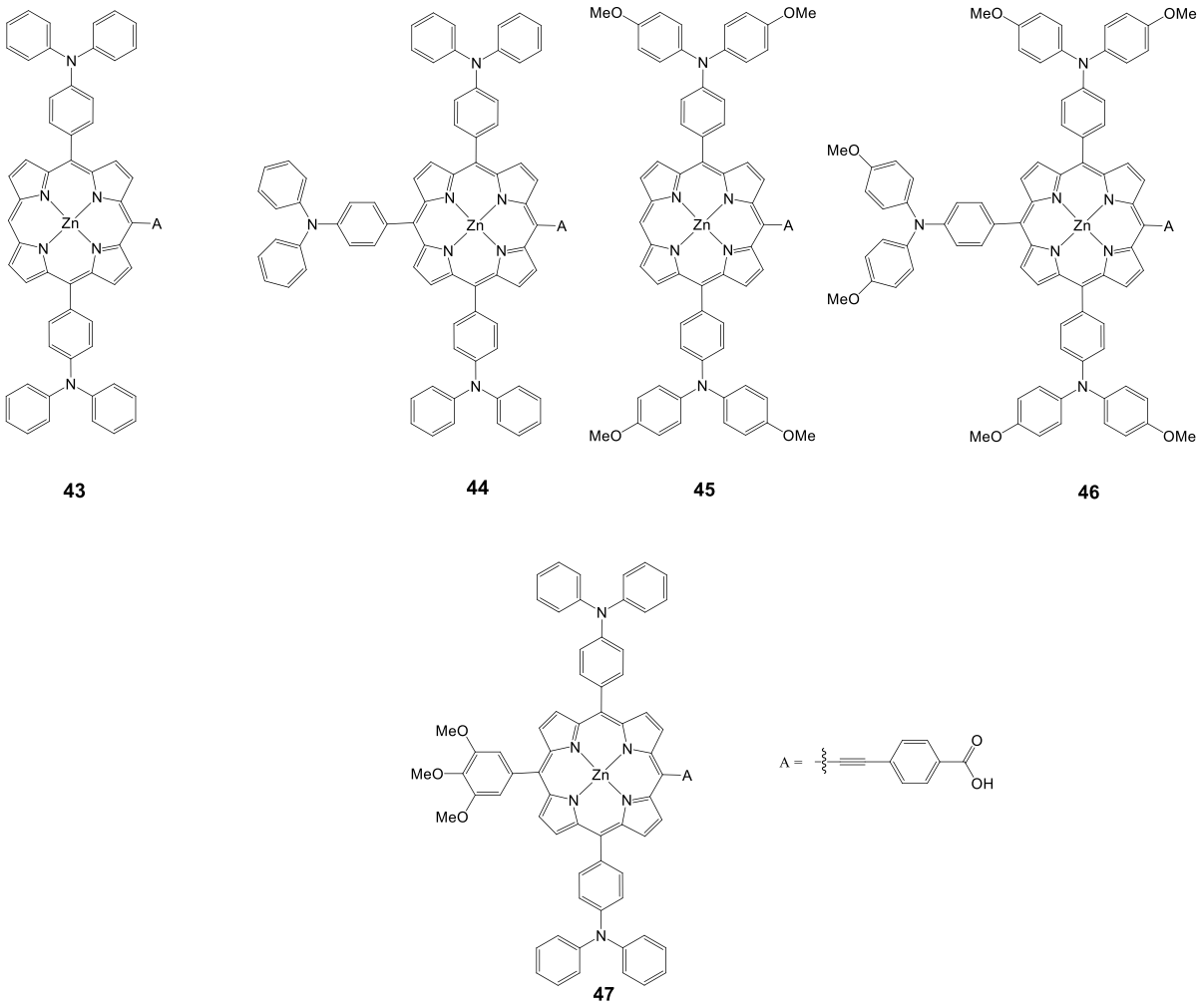

Figure 14. Molecular structures of **43-47**.

Table 6: Photovoltaic performances of DSSCs using **43-47** as sensitizers.

Dye	V_{oc}, mV	J_{sc}, mA cm^{-2}	FF	n, %
43	624	13.04	0.54	4.36
44	573	12.38	0.58	4.10
45	560	10.19	0.62	3.53
46	533	7.86	0.64	2.70
47	665	15.36	0.53	5.45

Following their research work on porphyrin dyes in order to improve the light harvesting properties, Imahori and coworkers demonstrated PCE of 10.1% (J_{sc} =19.33 mA/cm^2, V_{oc} = 0.72 V and FF =0.724) and 8.3 % (J_{sc} = 16.26 mA/cm^2, V_{oc} = 0.71 V and *FF* = 0.72) for **48** and **49**, respectively (Figure 15).[81] Compound **48** is an asymmetrically enhanced push-pull porphyrin bearing two dyarilamino groups at the *meso* position with a *cis* configuration.

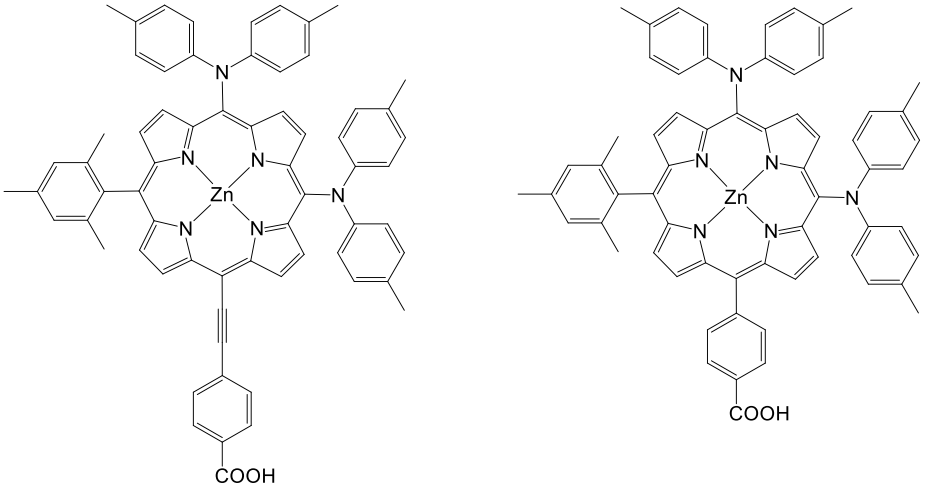

48 **49**

Figure 15. Molecular structure of dyes **48** and **49.**

Recently Lin *et al.*[82] prepared a series of new porphyrins (**50-53**) with near-IR light harvesting properties, for DSSCs, by attaching a pyrene or a 4-dimethylaminophenyl group in combination with anthracene to modify the porphyrin core (Figure 16). It was shown that the incorporation of these moieties renders feasible tuning of spectral and redox properties of the porphyrins. The PCE values of the dyes was in the range of 6.7 – 9.73 % and **50** sensitized DSSC showed a maximum PCE of 9.73 % (J_{sc} = 17.77 mA/cm^2, V_{oc} = 0.73 V and *FF* = 0.75), (Table 7). These high performances are due to the following factors (a) expansion of the porphyrin spectral range, (b) reduction of the dye aggregation bye suitable dye soaking processes, (c) addition of polar electron releasing groups.

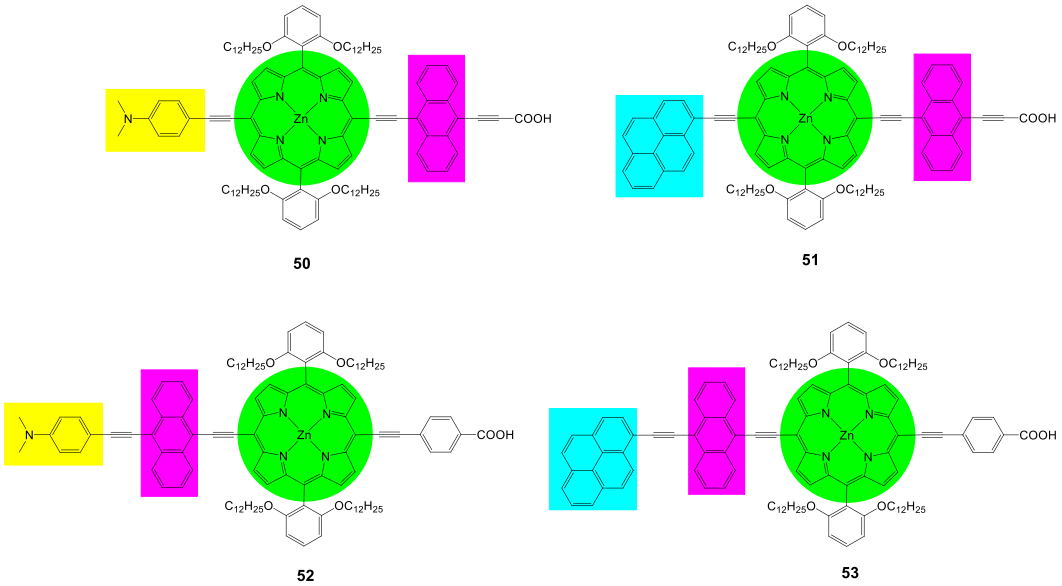

Figure 16. Molecular structures of dyes **50-53**.

Table 7: Photovoltaic performances[a] of DSSCs using **50-53** as sensitizers.

Dye	V_{oc}, mV	J_{sc}, mA cm^{-2}	FF	n, %
50	730	17.77	0.75	9.73
51	680	14.17	0.72	6.97
52	720	17.76	0.74	9.51
53	680	14.20	0.69	6.70

[a]Under AM1.5 illumination (power 100 mW cm^{-2}) with an active area of 0.096 cm^2.

2.2.2 *β*-Position Linking

The use of conjugated *β*-substituted anchoring groups was first demonstrated in 2004 by Grätzel *et al.* when they introduced a dye **54** with an energy conversion efficiency of 4.1% (J_{sc} = 8.86 mA/cm^2, V_{oc} = 0.65 V and *FF* = 0.71).[46] Also, for porphyrins with carboxylic binding groups, the Zn containing diamagnetic metalloporphyrins **63** and **55** had very high incident monochromatic photon-to-current conversion efficiencies compared to those observed for the Cu containing paramagnetic metalloporphyrin **56** (Figure 17, Table 8).

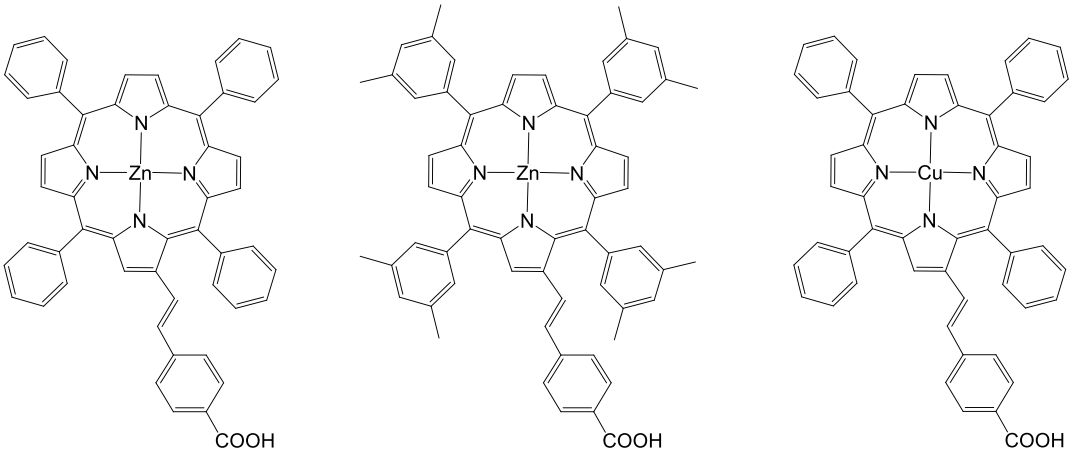

Figure 17. Molecular structures of porphyrins **54-56**.

Table 8: Photovoltaic performances of DSSCs using **54-56** as sensitizers.

Dye	V_{oc}, mV	J_{sc}, mA cm^{-2}	FF	n, %
54	654	8.86	0.71	4.11
55	660	9.70	0.75	4.80
56	490	1.35	0.69	0.45

In 2007, Officer and *co-workers* reported a series of porphyrins **57-62** with a conjugated bridge to a dicarboxylic acid acceptor moiety (Figure 18).[83] Porphyrin **58** gave the best efficiency 7.1% and the rest of the dyes featured efficiencies over 5% (Table 9).

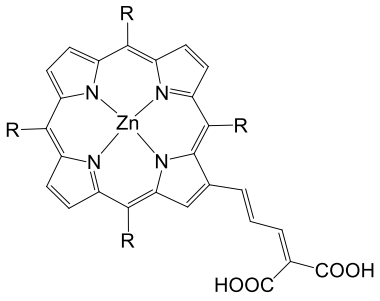

57: R=Ph
58: R=4-methylPh
59: R=4-ethylPh
60: R=4-*n*-butylPh
61: R=4-*n*-octylPh
62: R=3,5-dimethylPh

Figure 18. Molecular structures of dyes **57-62**.

Table 9: Photovoltaic performances[a] of DSSCs using zinc tetraarylporphyrin malonic acids as sensitizers.

Dye	V_{oc}, mV	J_{sc}, mA cm^{-2}	FF	n, %
57	638	12.1	0.66	5.1
58	680	14.0	0.74	7.1
59	642	14.8	0.63	5.8
60	701	13.4	0.68	6.4
61	649	13.4	0.61	5.3
62	685	13.3	0.68	6.1

[a] Data obtained under cell illumination AM 1.5. 100mW/cm^2.

Since the 2007 report on *β*-linked porphyrins, Officer and *coworkers* used *β*-linked derivatives to study several aspects of solar cell design and performance. The aspects of design under study included the use of a post adsorbed phosphinic acid blocking moiety to improve efficiencies by minimizing recombination events at the electrode surface.[84] They also studied the use of ionic liquid electrolytes as a replacement for volatile organic solvents in typical liquid electrolytes.[85] The Officer group had also studied the open-circuit voltage and electron injection dynamics using *β*-substituted porphyrins and suggested that the reason for limitations to the V_{oc} and J_{sc} were related to reduced electron lifetime and less favorable electron injection dynamics.[86,87]

Porphyrins (**63**-**70**) functionalized at *meso*- and *β*-positions with different carboxylic acid groups were prepared to investigate the photovoltaic properties as dye sensitized nanocrystalline-TiO_2 solar cells (Figure 19).[88] The electronic structures of the porphyrin macrocyclic core were strongly coupled with olefinic side chains so that the absorption spectrum exhibited largely broad and red-shifted Soret and Q-bands. In the case of the doubly functionalized porphyin with malonic di-acid groups, the Soret band appeared at 475 nm.. Among porphyrin derivatives prepared in this study, compound **70** exhibited the maximum overall conversion efficiency of 3.03% (Table 10). From

such photovoltaic performances, it was suggested that multiple pathways through olefinic side chains at two β-positions enhanced the overall electron injection efficiency and the moderate distance between the porphyrin sensitizer and the TiO_2 semiconductor layer was important, retarding the charge recombination processes. As a consequence, these combined effects gave rise to higher photovoltaic efficiency in photovoltaic regenerative solar cells.

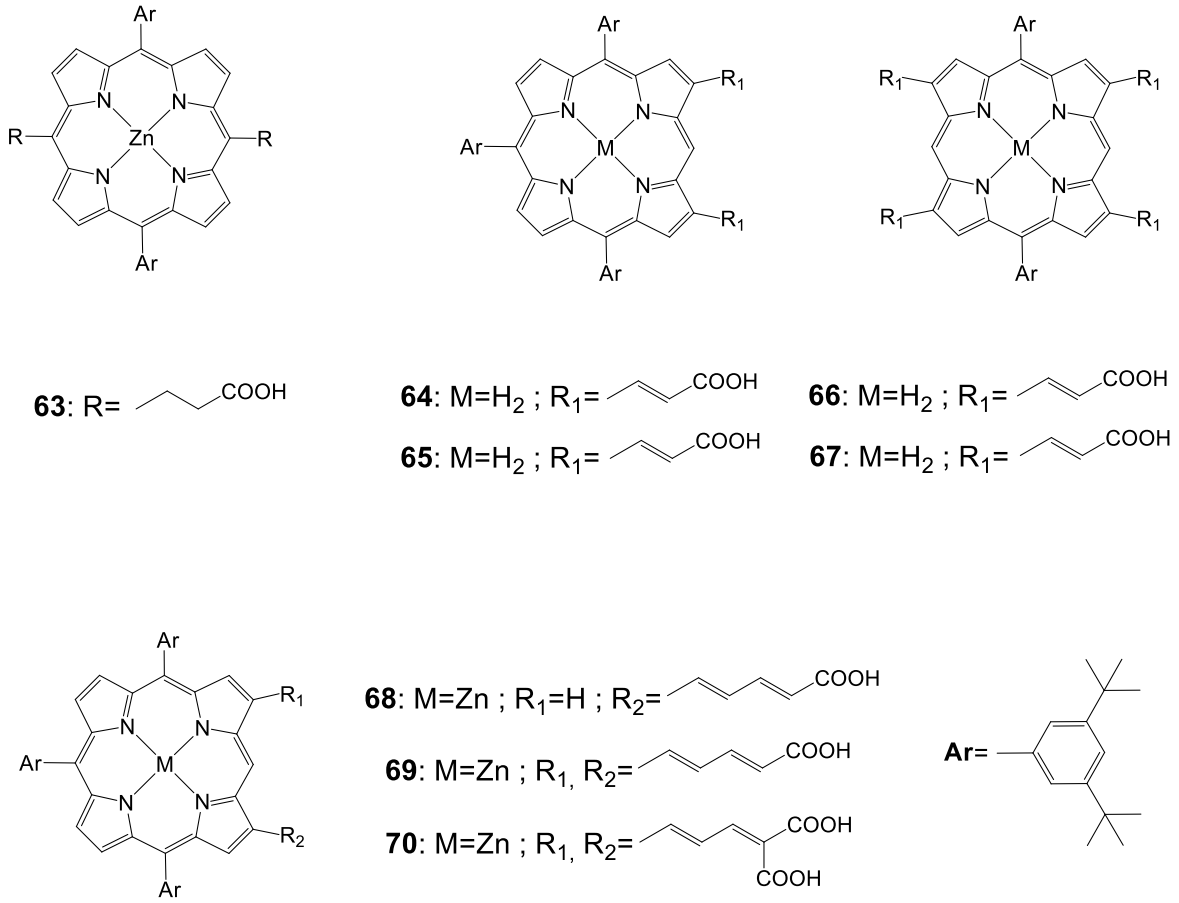

Figure 19. Molecular structures of porphyrins **63-70**.

Table 10: Photovoltaic performances[a] of DSSCs using **63-70** as sensitizers.

Dye	V_{oc}, mV	J_{sc}, mA cm^{-2}	FF	n, %
63	450	0.51	0.60	0.14
64	510	1.84	0.67	063

65	540	4.45	0.61	1.48
66	b	b	b	b
67	b	b	b	b
68	540	6.20	0.62	2.08
69	560	6.74	0.62	2.37
70	590	8.38	0.62	3.03

[a]Overall conversion efficiency parameters were measured in the light condition of 100 mW cm^{-2} illumination. [b] Not measured.

In 2011 three porphyrins with structures based on a molecular design that relies on donor-π-acceptor interactions (Figure 20).[89] At the *meso* position of the porphyrin was present a *bis* (4-tert-butylphenyl) amino group and at the opposite side were 2-propenoic or 2,4-pentadienoic acid anchoring groups at the β-pyrrolic positions. The efficiencies of all compounds are present in Table 11 and among the dyes prepared, the doubly functionalized carboxylic acid derivative **73** gave rise to the highest power conversion with an efficiency of 7.47%.

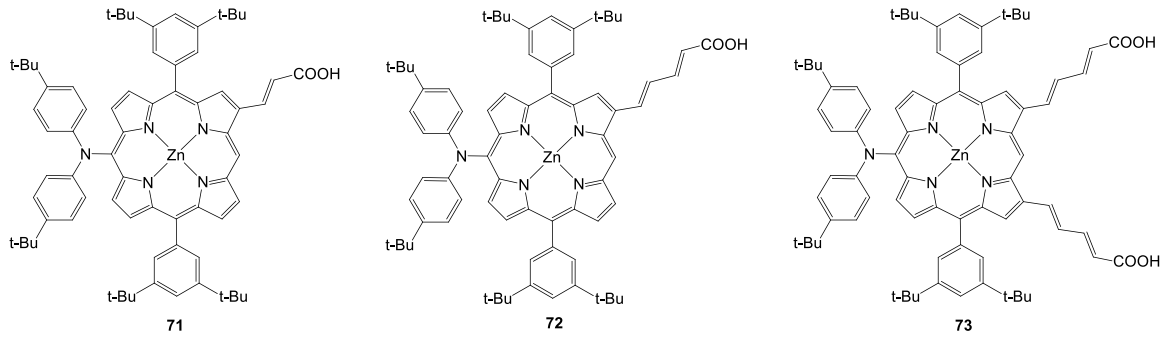

Figure 20. Molecular structures of porphyrins **71-73**.

Table 11. Photovoltaic performance of DSSCs using porphyrins **71-73** as sensitizers.

Dye	J_{sc}, mA cm^{-2}	V_{oc}, mV	FF	n, %
71	12.1	660	0.62	4.95
72	13.9	670	0.64	5.91
73	18.4	710	0.57	7.47

In another study following the same concept of push–pull, two *meso*-di-substituted porphyrinic dyes **74** and **75** (Figure 21) were synthesized followed a facile route in order to compare the efficiency between them.[90] It was found that the performance of DSSCs based on *β*-di-substituted push–pull dye **74** was measured to be slightly superior 4.1% (J_{sc} = 11.6 mA/cm^2, V_{oc} = 0.56 V and *FF* = 0.62)to this of DSSCs based on *meso*-bi-substituted dye **75** 3.9% (J_{sc} = 11.1 mA/cm^2, V_{oc} = 0.60 V and *FF* = 0.59).

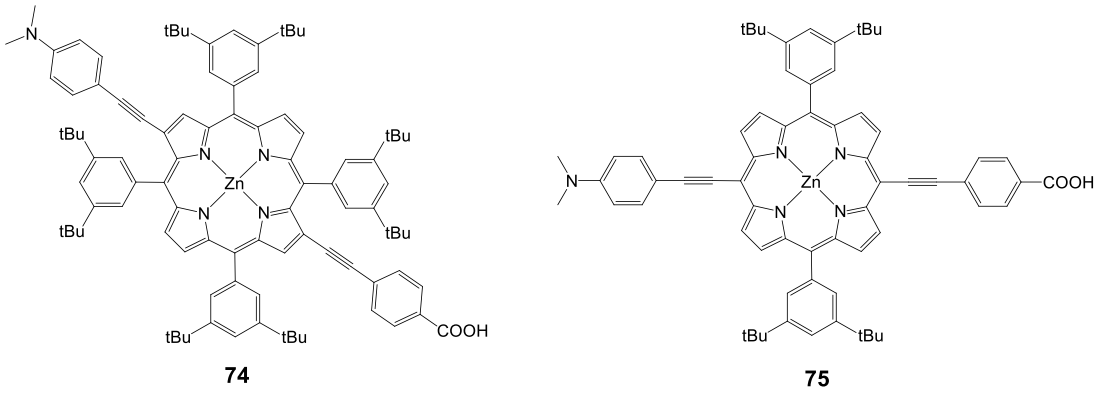

Figure 21. Molecular structures of compounds **74** and **75**.

Moreover, a very interesting study compared silatrane, phosphonic acid, and carboxylic acid functional groups (Figure 22) for attachment of porphyrin sensitizers to TiO_2 in photoelectrochemical cells. Porphyrin sensitizers bearing *β*-vinyl substituents with carboxylic acid **76**, phosphonic acid **77**, or silatrane moieties **78** had similar photophysical properties.[91] All three molecules could be attached to nano-particulate anatase TiO_2 by soaking in an appropriate solvent, but about twice the surface coverage

was obtained with the carboxylic acid, relative to the other two linker groups. Maybe this was due to differences in the geometry of the anchoring groups on the oxide surface. In DSSCs, V_{oc} and *FF* were comparable for all three linkers, but the short-circuit current and solar conversion efficiency of the cell with the carboxylic acid linked sensitizer were about twice those observed with the phosphonic acid and silatrane linkers. Thus the photoelectrochemical parameters for all three sensitizers were comparable, but the carboxylic acid bearing sensitizer gave about twice the solar conversion efficiency because of the increased surface coverage (Table 12). This was due to increased light absorption, absorption closer to the electrode FTO conducting surface and increased surface passivation. On the other hand, the carboxylate linkage was readily hydrolyzed, especially under basic conditions, resulting in loss of the sensitizer from the surface. Phosphonate linkages were much less labile, and the siloxyl linkages derived from the silatrane treatment were the most resistive to hydrolysis under the conditions examined. Such resistance to cleavage was important for long term stability of DSSCs, and especially for photoelectrochemical cells with aqueous electrolytes that were used for light-powered water oxidation and fuel production.

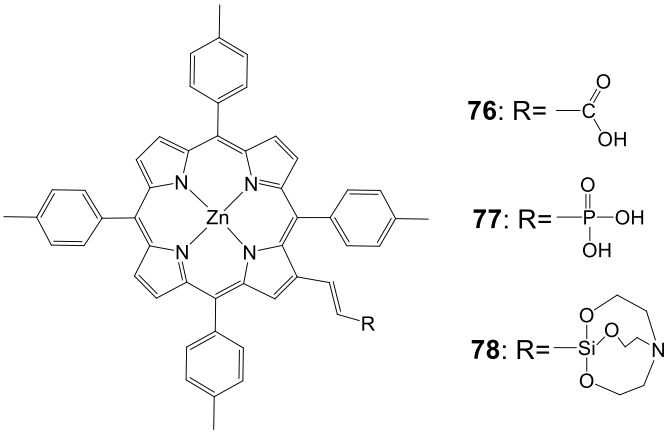

Figure 22. Molecular structures of dyes **76-78.**

Table 12. Photovoltaic performance [a] of DSSCs using porphyrins **76-78** as sensitizers.

Dye	J_{sc}, mA cm^{-2}	V_{oc}, mV	FF	n, %
76	2.49	444	0.52	0.57
77	1.11	426	0.53	0.25
78	1.10	423	0.53	0.25

[a]Illuminated using simulated AM1.5G sunlight at 1000 W m^{-2}.

2.2.3 Cyanoacrylic Acids

Another anchoring group that has been extensively used is the cyanoacrylic acid. In 2005, tetraphenylporphyrin with a β-substituted cyanoacrylic acid (Figure 23), exhibited an efficiency of 5.2% (J_{sc} = 13.5 mA/cm^2, V_{oc} = 0.56 V).[44] Dye **79** had a better efficiency compared to the carboxylic acid porphyrin **81** 4.0% (J_{sc} = 10.9 mA/cm^2, V_{oc} = 0.55 V), synthesized from the same group.

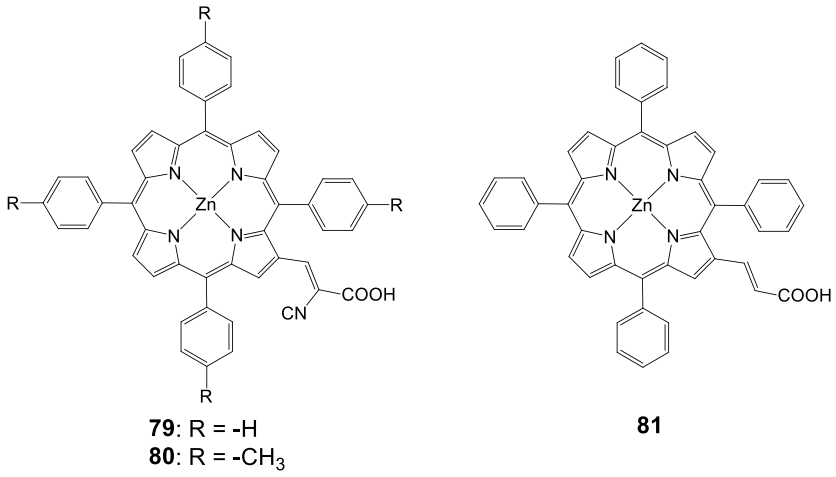

Figure 23. Molecular structures of dyes **79-81**.

In another study β-substituted zinc porphyrin analogues **79** and **80** (Figure 23) were synthesized, where **80** had an added methyl group at the phenyl ring attached to the meso-position of the porphyrin macrocycle.[92] These results showed that the different solvents used in the sensitization process affected how the dyes were aggregated and how much of the dyes were adsorbed on the semiconductor surface. The highest efficiency of 4.2% (J_{sc} = 13.0 mA/cm^2, V_{oc} = 0.48 V and FF = 0.67), 30 min soaking time and 4.0% (J_{sc} = 12.8 mA/cm^2, V_{oc} = 0.46 V and FF = 0.67), 1 hour soaking

time was achieved for **79** and **80** analogues, respectively. The difference in the photovoltaic properties between **79** and **80** was caused by the amount of tilting of the molecular dye plane toward the dye surface. The **80** molecular planes were closer to the TiO_2 surface due to the increased steric effect caused by the addition of a methyl group (Figure 24). This increased the surface area of the dye adsorbed in the TiO_2, resulting a much lower dye concentration. The soaking condition and the use of co-adsorbents giving much higher photovoltaic performances could control the amount of aggregation of the dye.

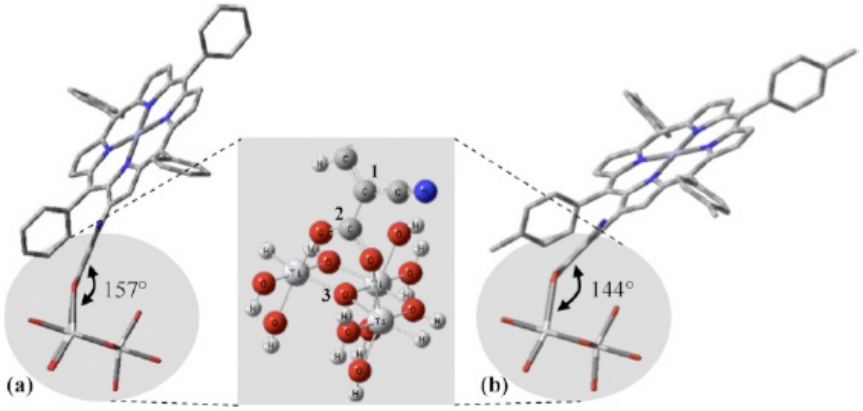

Figure 24. Possible adsorption configurations of (a) **79** and (b) **80**. The inset shows the bidentate adsorption of the dye. C1–C2–O3 determines the dye molecular angle against the TiO_2. Adapted from Ref. 92

Research by Liu *et al*. was focused on adding thiophenyl groups to the *para*-position of *meso*-phenyl groups with and without a specific binding functionality (*i.e.* –COOH). Dye **82** (Figure 25) gave an efficiency of 5.1% (J_{sc} = 12.9 mA/cm^2, V_{oc} = 0.60 V and *FF* = 0.66) when DMF was used as the adsorption solvent.[93]

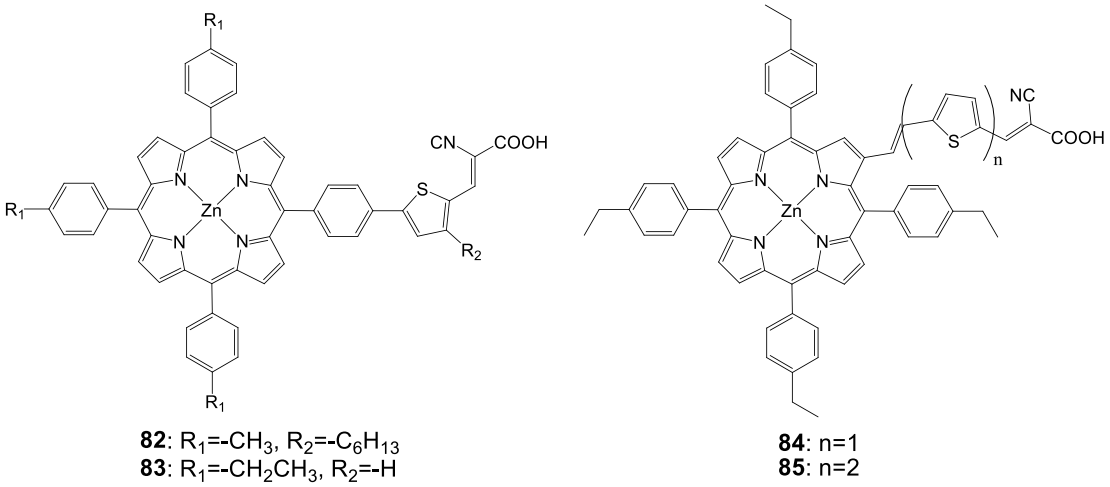

Figure 25. Molecular structures of porphyrins **82-85**.

In order to explore the nature of the linker between the porphyrin and the anchoring group, *β*-substituted porphyrins **83, 84** and **85** (Figure 25) containing thiophene linker and ethyl group on *meso*-phenyl group were synthesized and studied their photoelectronic properties (Table 13).[94] The results of this study showed that **84** and **85** had a tendency to undergo aggregation due to their almost planar structure (Figure 26), which resulted to the reduced cell efficiency. However, the bent structure of **83** was able to suppress the aggregation. The low binding ability of **83** could be explained due to the shorter length of linker and bent structure. Porphyrin ring plane of **83** was largely bent from the linker group, leading to steric hindrance between porphyrin moiety and surface of TiO_2.

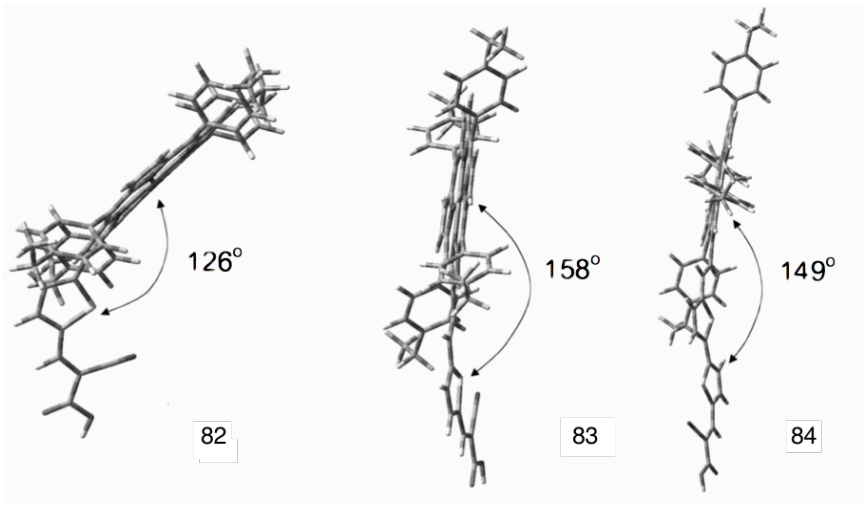

Figure 26. Optimized structures of dyes **82**- **84**. Adapted from Ref.94.

Table 13. Photovolataic performances of DSSC using **83**-**85**.

Dye	J_{sc}, mA cm^{-2}	V_{oc}, V	FF	n%
83	1.6	0.49	0.67	0.5
84	11.8	0.60	0.64	3.2
85	13.0	0.61	0.66	4.0

To improve the absorption profile of the porphyrin dyes towards longer wavelength region, it was reported that π-extended porphyrins[27] and accessory pigment attached porphyrin[95] that enhances their absorption profile in red region of the solar spectrum. Additionally, using four anchoring groups instead of one anchoring unit, improves the performance of the DSSCs.[55] Hupp *et al.* have employed a π-extended porphyrin possessing two anchoring units **87** as sensitizer and achieved a superior PCE of 5.5 % (J_{sc} = 11.3 mA/cm^2, V_{oc} = 0.68 V and *FF* = 0.70) compared to **86** (3.5 %, J_{sc} = 7.5 mA/cm^2, V_{oc} = 0.66 V and *FF* = 0.69) sensitized solar cell (Figure 27).[96]

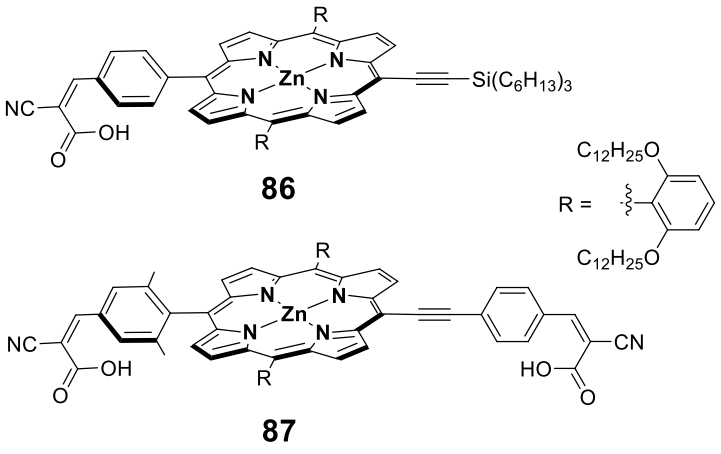

Figure 27. Molecular structures of compounds **86** and **87**.

New β-pyrrolic functionalized porphyrins with donor–*p*–acceptor character were synthesized and characterized as dye sensitizers for DSSCs (Figure 28).[97] Two types of *p*-conjugated spacers, namely benzene and thiophene rings, with cyanoacrylic acid as an acceptor were linked to the porphyrin ring at the β-pyrrolic position. These porphyrins

showed high thermal and electrochemical stability. As sensitizers, the porphyrin dye bearing a thiophene ring as the *p*-conjugated spacer **88** gave better cell performance with an overall conversion efficiency of 1.94% (J_{sc} = 4.57 mA/cm^2, V_{oc} = 0.59 V and *FF* = 0.59), compared to a 1.13% (J_{sc} = 2.62 mA/cm^2, V_{oc} = 0.59 V and *FF* = 0.57)for dye **89**.

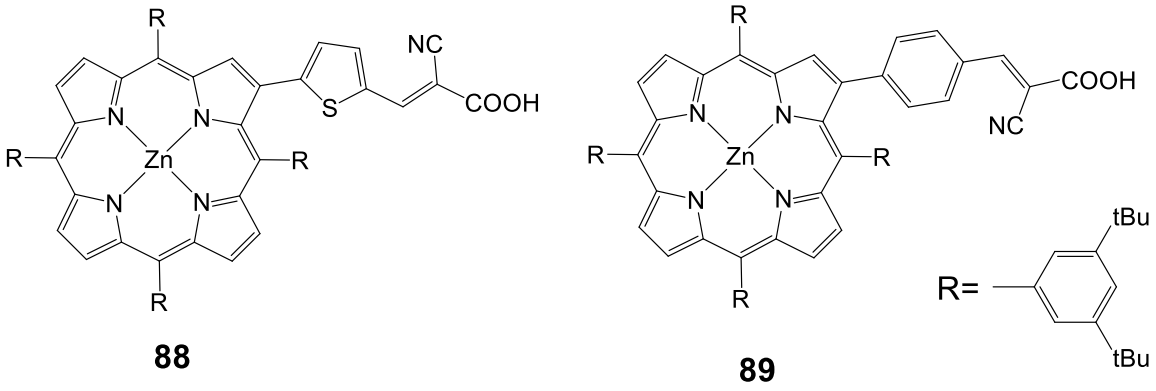

Figure28. Molecular structures of porphyrins **88** and **89**.

In another study porphyrins were synthesized with a push-pull orientation bearing cyanoacrylic acid in the *β* **90** and *meso* positions **91** of the porphyrin ring (Figure 29).[90] The "pull" ethynylphenyl substituent bearing the cyanoacrylic acid group in the *β* position had a higher efficiency 4.7% (J_{sc} = 14.0 mA/cm^2, V_{oc} = 0.59 V and *FF* = 0.58) over 4.2% (J_{sc} = 13.3 mA/cm^2, V_{oc} = 0.52 V and *FF* = 0.61). In the same study it was observed that the critical factor in determining injection efficiency in *β*-substituted DSSCs was the chemical nature of the anchoring group, with the cyanoacrylic acid group exhibiting a better performance than the carboxylic group of a benzoic acid moiety, confirming the findings of another report.[98]

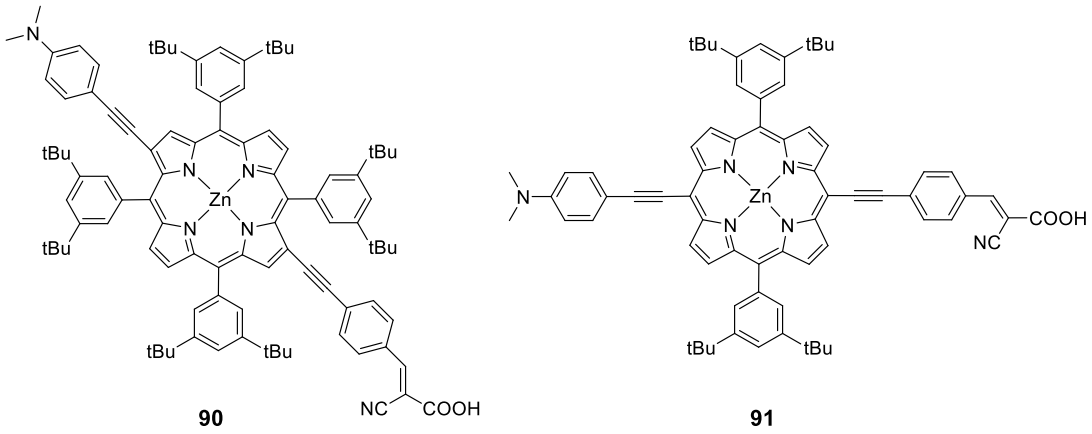

Figure 29. Molecular structures of dyes **90** and **91**.

In other work, three push-pull structured new porphyrin dyes with various linkers (the **92** dye with 4-ethynylbenzene, the **93** dye with 2-ethynylthiophene, and the **94** dye with 5-ethynyl-2,3-dihydrothieno[3,4-b][1,4]dioxine) were synthesized in order to understand the influence of substitution of the *p*-linker with various hetero-aromatic groups (Figure 30) on the light-harvesting ability of the sensitizers.[99] These push–pull structured porphyrin sensitizers worked efficiently in DSSC devices, a detailed examination with impedance and transient photovoltage decay measurements revealed that a fast recombination process took place at the dye-sensitizer TiO_2–electrolyte interface due to the introduction of cyanoacrylic acid as an anchoring group. Based on these studies the **95** porphyrin with a rigid π-linker feature structure (5-ethynylthiophene-2-carboxylic acid) was further designed and synthesized, which attained an improved PCE of 9.53% (Table 14).

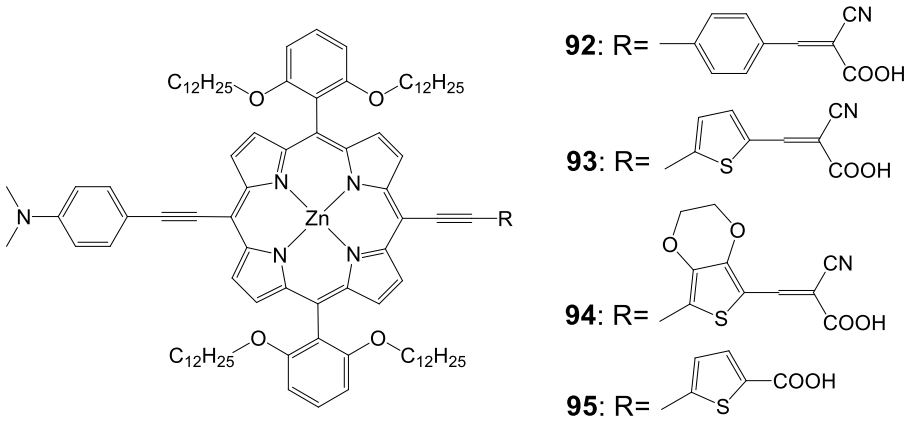

Figure 30. Molecular structures of compounds **92-95**.

Table 14. Photovolataic performances of DSSC using **92-95**.

Dye	J_{sc}, mA cm^{-2}	V_{oc}, V	FF	n%
92	15.70	0.648	0.70	7.12
93	15.36	0.685	0.70	7.37
94	16.35	0.657	0.71	7.63

95	17.65	0.75	0.72	9.53

A series of push-pull structured (D-π-A) porphyrin dyes with an electron donating group attached at the *meso* position (**96-98**) were designed by Kim *et al.*[100] for the use of sensitizers for DSSCs (Figure 31). The absorption bands of these porphyrin dyes were broadened and red shifted upon introduction of alkoxy chains to the electron donating groups at *meso* position opposite to the anchoring cyanoacrylic acid group. Among the sensitizers, the highest PCE of DSSC fabricated with **98** was 4.7 % (J_{sc} = 11.8 mA/cm^2, V_{oc} = 0.593 V and *FF* = 0.651) and further improved up to 7.6 % (J_{sc}= 15.9 mA/cm^2, V_{oc} = 0.68 V and *FF* = 0.703) when **99** used as coadsorbent (Table 15).

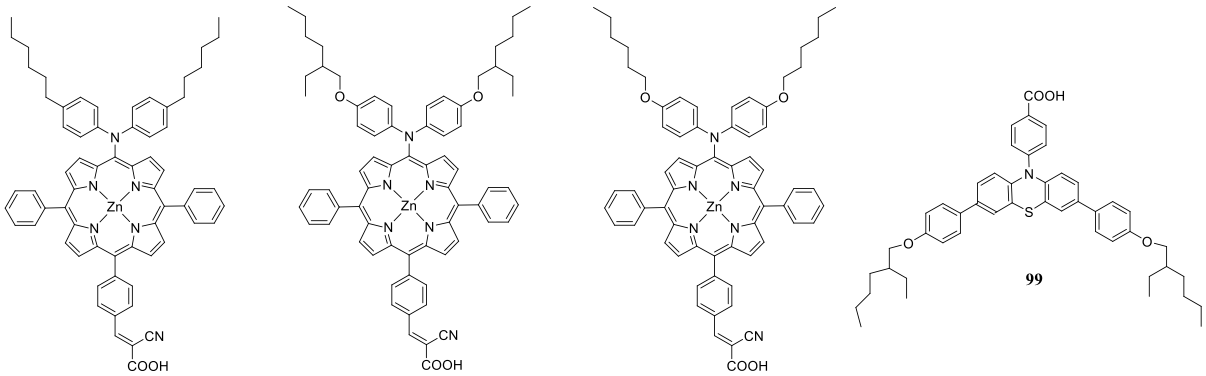

Figure 31. **Molecular structure of compounds** 96-98 **and coadsorbant** 99**.**

Table 15. Photovolataic performances of DSSC using **96-98**.

Dye	J_{sc}, mA cm^{-2}	V_{oc}, V	FF	*n*%
96	4.9 (10.9)[a]	0.546 (0.593)	0.74 (0.77)[a]	2.0 (5.0)[a]
97	9.6 (13.4)[a]	0.548 (0.632)[a]	0.69 (0.72)[a]	3.6 (6.1)[a]
98	11.8 (15.9)[a]	0.617 (0.678)[a]	0.65 (0.70)	4.7 (7.6)[a]

[a]Compound **99** was used as the co-adsorbent.

Kim *et al.* designed two Zn(II)-porphyrin sensitizers (**100** and **101** with a bulky alkoxy group in order to retard the charge recombination (Figure 32).[101] The DSSCs

sensitized **100** and **101** showed a PCE of 4.88 % (J_{sc}= 10.92 %, V_{oc} = 0.63 % and *FF* = 0.71) and 4.53 % (J_{sc}= 10.36 %, Voc= 0.60% and FF= 0.73), respectively. Moreover, when **104** incorporated into the dye solution as coadsorbant, the PCE has been enhanced significantly up to 8.46 % (J_{sc}= 15.39 mA/cm^2, V_{oc} = 0.74 V, *FF*= 0.74) for **100** and 7.02 % (J_{sc}= 13.72 mA/cm^2, V_{oc} = 0.686 V, *FF* = 0.75) for **101** (Table 16).

The same research group also synthesized two D-π-A structured Zn(II) porphyrin dyes **102** and **103** containing an electron donating bis(3,3-dimethylfluorenyl)amine moiety at the *meso* position and different carboxylic acid and cyanoacrylic acid at the opposite meso position linked through a phenylene π-conjugation bridge.[33] The DSSCs sensitized with **102** and **103** showed PCE of 3.16 % (J_{sc} = 7.37 mA/cm^2, V_{oc} = 0.56 and *FF* = 0.77) and 4.37 % (J_{sc} = 10.04 mA/cm^2, V_{oc} = 0.58 V and FF = 0.75), respectively. The PCE of **102** sensitized was improved up to 7.22 % (J_{sc}= 15.30 mA/cm^2, V_{oc} = 0.67 V and *FF* = 0.71) when the 0.1mM **104** was used as coadsorbant (Table 16). These results clearly demonstrate that efficient intra-molecular charge separation of D-π-A Zn(II) porphyrin can by induced by inserting a strongly electron accepting cynanoacrylic acid substituents, resulting an relatively high overall PCE.

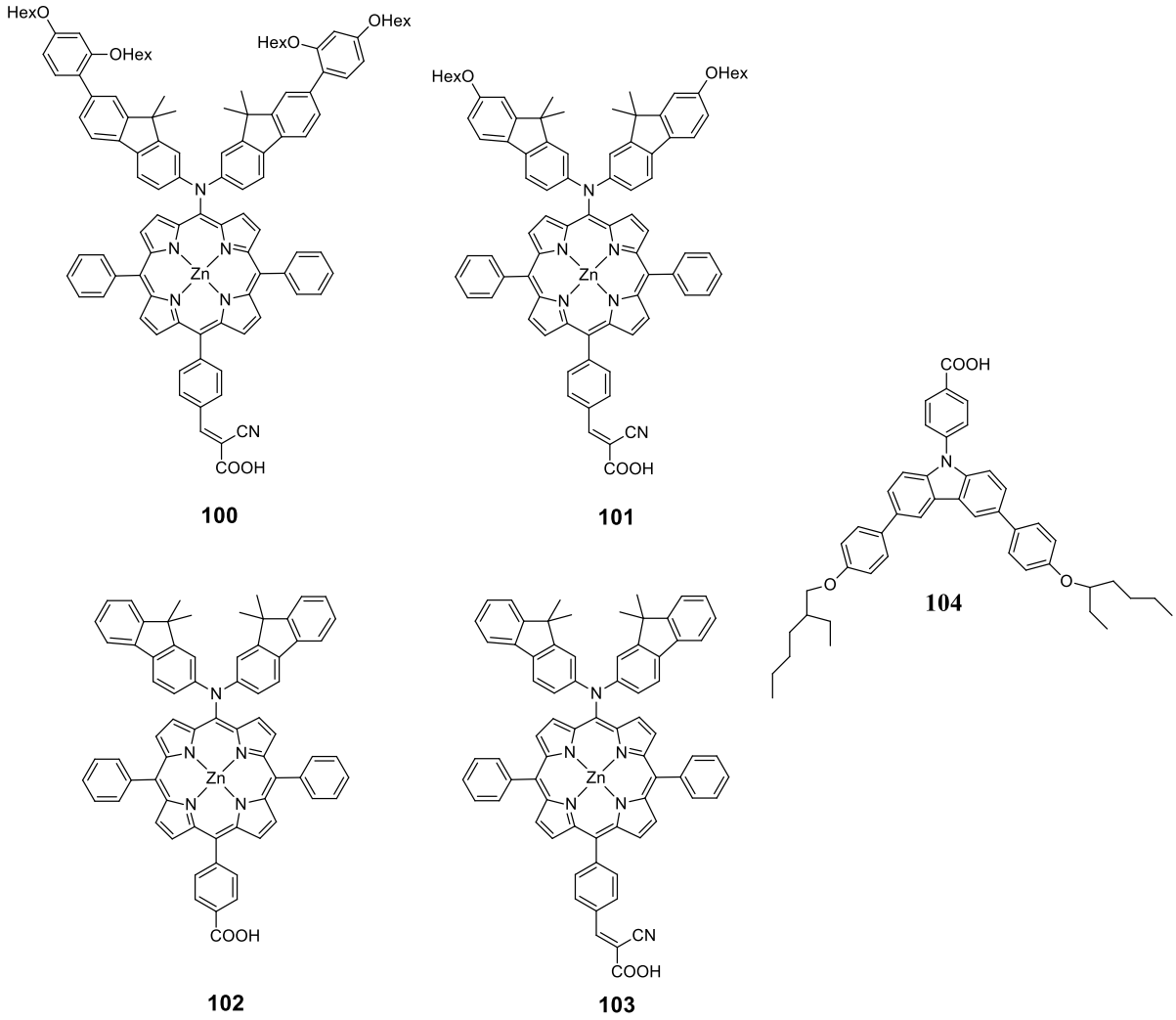

Figure 32. Molecular structure of dyes **100**-**103** and coadsorbant **104**.

Table 16. Photovolataic performances of DSSC using **100**-**103**.

Dye	J_{sc}, mA cm^{-2}	V_{oc}, V	FF	*n*%
100	10.92 (15.39)[a]	0.63 (0.74)	0.71 (0.74)[a]	4.88 (8.46)[a]
101	10.36 (13.72)[a]	0.60 (0.686)[a]	0.73 (0.75)[a]	4.53 (7.02)[a]
102	7.37 (15.30)[a]	0.56 (0.67)[a]	0.77 (0.71)	3.16 (7.22)[a]
103	10.04 (14.59)[a]	0.58 (0.63)[a]	0.75 (0.72)	4.37 (6.64)[a]

[a]Compound **104** was used as the co-adsorbent.

Diau and Yeh[102] synthesized *p*-extended porphyrin dye**105** and **106** with long alkoxyl chains at the *ortho* positions and cyanoacrylic acid as an anchoring group

(Figure 33). The efficiencies of both compounds were quite poor 5.8% (J_{sc} = 11.30 mA/cm^2, V_{oc} = 0.69 V and FF = 0.74) for **105** and 3.6% (J_{sc} = 7.17 mA/cm^2, V_{oc} = 0.67 V and FF = 0.75) for **106**. This was due to the floppy structural nature and limited molecular rigidity of the cyanoacrylic acid anchor, which might lead the porphyrins to tilt down the TiO_2 surface for an efficient charge recombination to occur.[103,104]

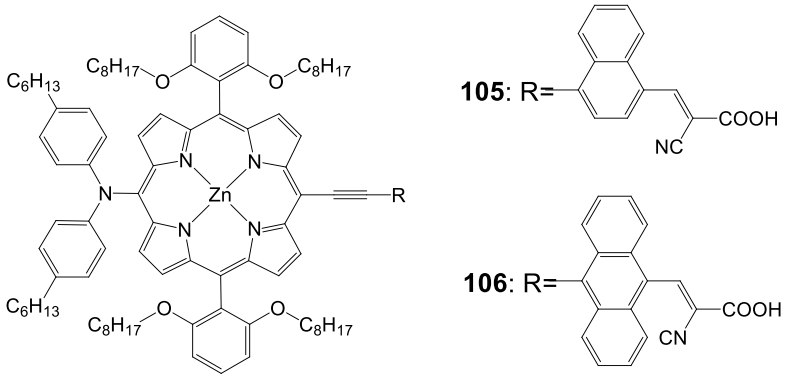

Figure 33. Molecular structure of dyes **105** and **106**.

2.3 Fused Porphyrins

One issue with porphyrins as sensitizers in DSSCs is their limited absorptivity in the red and near infrared regions of the solar spectrum. With *meso*-tetraphenylporphyrins the phenyl moieties are typically considered perpendicular to the plane of the macrocycle and therefore are not in conjugation with the porphyrin system. One design strategy for increasing the light absorption of porphyrin sensitizers is to lock the *meso*-phenyl ring into the plane of the macrocycle in order to improve the conjugation between the porphyrin and the phenyl rings. This strategy has the added benefit of increasing the molecular asymmetry of the molecule. The combination of added conjugation and increased molecular asymmetry manifests itself as a red shift in the absorption spectrum of the molecule. The following examples synthesized towards this strategy.

One way to improve the light harvesting property of porphyrin sensitizers is to introduce the unsymmetrical π-elongation in the porphyrins.[27,62,105-110] Imahori and coworkers reported novel *β*-linked porphyrins **107** and **108** (Figure 34) with carboxyquinoxalino or dicarboxyquinoxalino moieties respectively.[106] Compound **107** gave a solar energy conversion efficiency of 5.2% (J_{sc} = 11.2 mA/cm^2, V_{oc} = 0.72 V and FF

= 0.68)in a standard DSSC, while the dicarboxy derivative **108** gave 4% (J_{sc} = 9.3 mA/cm^2, V_{oc} = 0.67 V and FF = 0.64) efficiency. The superior performance of the **107**-sensitized solar cell to the **108**-sensitized one was originated from both the more favorable electron injection and charge collection efficiency.

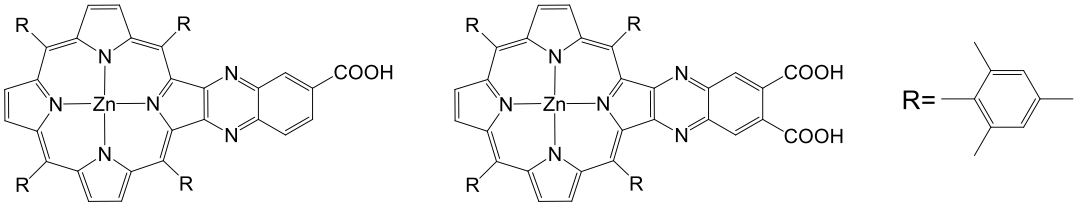

107 **108**

Figure 34. Molecular structure of dyes **107** and **108**.

The same group synthesized unsymmetrical π-elongated porphyrins (Figure 35), in which the naphthyl moiety was fused to the porphyrin core at the naphthyl bridge with a carboxyl group **109** or at the opposite side of the phenyl bridge with a carboxyl group **110**.[109] The **109** and **110**-sensitized TiO_2 solar cells showed the power conversion efficiencies (n) of 4.1% (J_{sc} = 10.6 mA/cm^2, V_{oc} = 0.62 V and FF = 0.62) and 1.1% (J_{sc} = 3.6 mA/cm^2, V_{oc} = 0.53 V and FF = 0.58), respectively, under standard AM 1.5 conditions. The n value of the **109** cell was improved by 50% compared to the reference cell using unfused porphyrin **111**. The **109**-sensitized cell revealed high IPCE values of up to 55%, extending the response of photocurrent generation close to 800 nm. Thus, the improved photocurrent generation of the **109**-sensitized cell relative to the **111**-sensitized reference cell was responsible for the remarkable difference in the η values. The n value of the **110** cell was much lower than that of the **109** cell. DFT calculations disclosed that there were significant electron densities on the carboxyl group in the LUMO of **109**, whereas there were little electron densities on the carboxyl group in the LUMO of **110**. Accordingly, the larger electronic coupling between the porphyrin and the TiO_2 surface in the **109**-sensitized cell may be responsible for the high cell performance, due to the efficient electron injection from the porphyrin excited singlet state to the conduction band of the TiO_2 electrodes. To further improve the cell performance, porphyrin **4**, possessing different light-harvesting properties, was co-adsorbed with **109** onto a TiO_2 electrode. Under the optimized conditions, the cosensitized cell yielded IPCE value of 86%, short circuit photocurrent density of 11.7

mA cm^{-2}, open-circuit voltage of 0.67 V, fill factor (FF) of 0.64, and *n* of 5.0% under standard AM 1.5 conditions (Table 17).

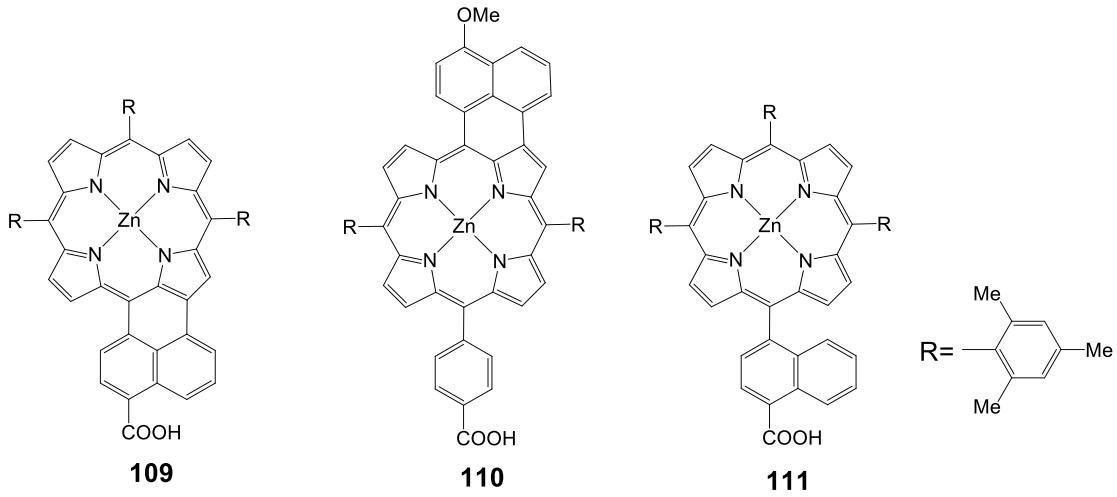

Figure 35. Molecular structure of porphyrins **109-111**.

Table 17. Photovolataic performances of DSSC using **109**-**111**.

Dye	J_{sc}, mA cm^{-2}	V_{oc}, mV	FF	*n*%
109	10.6	620	0.62	4.1
110	3.6	530	0.58	1.1
111	6.7	610	0.68	2.8

New *opp*-dibenzoporphyrins (Figure 36) were synthesized through a Pd^0-catalyzed cascade reaction.[111] These *opp*-dibenzoporphyrins (**112**-**116**) were evaluated for the first time as light harvesters for dye-sensitized solar cells. These porphyrins displayed moderate solar energy-to-electricity conversion efficiencies of 1.54–3.14%. The installation of a more bulky group on the *meso*-phenyl rings of the porphyrin did not help to enhance the solar-energy conversion, presumably owing to lower adsorption of the porphyrin dye on the TiO_2 surface. The incorporation of conjugated carboxylic acid linkers onto the porphyrin considerably broadened and red-shifted the

absorption bands of the porphyrin, thereby led to a very high J_{SC} value (12.89), (Table 18).

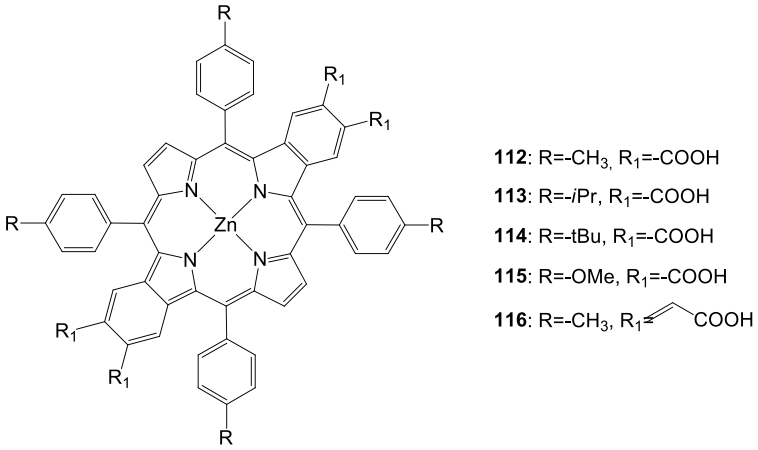

Figure 36. Molecular structure of dyes **112-116**.

Table 18. Photovolataic performances of DSSC using **112-116**.

Dye	J_{sc}, mA cm^{-2}	V_{oc}, V	FF	n%
112	8.86	0.57	0.58	2.93
113	5.05	0.54	0.56	1.54
114	5.52	0.58	0.57	1.81
115	7.48	0.57	0.53	2.22
116	12.87	530	0.46	3.14

A push-pull porphyrin **117** was synthesized and studied with an electron donating triarylamino group at the *β,β'*-edge through a fused imidazole group and an electron withdrawing carboxyquinoxalino anchoring group at the opposite *β,β`*-edge (Figure 37) and employed as sensitizer for DSSC. [112] The **117**-sensitized solar cell exhibited a relatively high PCE of 6.8% (J_{sc} = 13.9 mA/cm^2, V_{oc} = 0.68 V and FF = 0.71), which was larger than that of the **107**-sensitized solar cell 6.3% (J_{sc} = 13.2 mA/cm^2, V_{oc} = 0.71 V and FF = 0.67) with chenodeoxycholic acid as co-absorbent, to reduce porphyrin aggregation on TiO_2. The short-circuit current and FF of the **117**-sensitized

solar cell were larger than those of the **107**-sensitized solar cell, whereas the open circuit potential of the **117**-sensitized cell was smaller than that of the **107**-sensitized cell, leading to an overall improved cell performance of **117**.

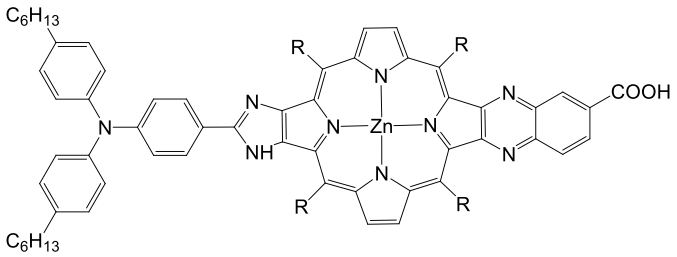

117

Figure 37. Molecular structure of dye **117**.

Yeh and coworkers[102] synthesized *p*-extended porphyrin dyes **118** and **119** with long alkoxyl chains at the *ortho* positions of the *meso* phenyls, and *meta* di-*tert*-butylphenyl-substituted porphyrins for DSSCs; their optical, electrochemical and photovoltaic properties were investigated and compared with those of **120** and **121** (Figure 38).

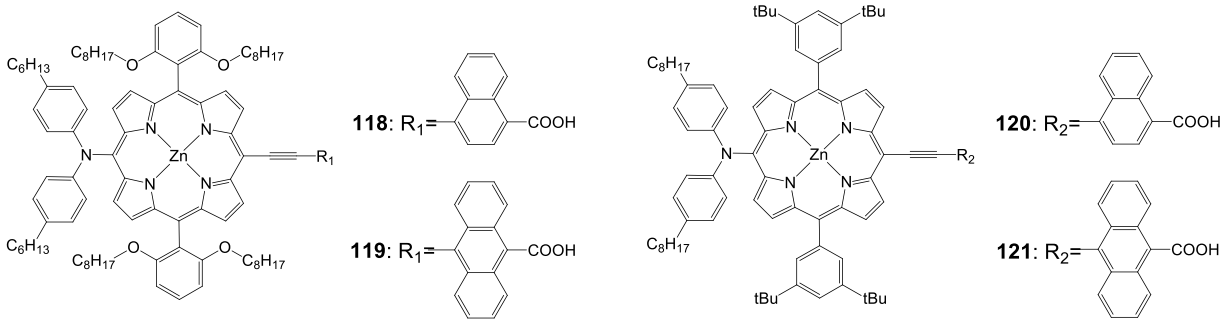

Figure 38. Molecular structure of dye **118-121**.

For the naphthalene-bridged porphyrins, the *ortho*-substituted long alkoxyl chains in the two *meso*-phenyls of **118** played a key role to prevent dye aggregation so that both J_{SC} and V_{OC} were significantly enhanced for **118** than for **120**. As a result, the PCE of **118** reached 8.04%, which was ~11% higher than that of **120** (7.23%). The devices made of **121** were found to perform extremely poorly due to a serious problem of dye aggregation on the TiO_2 surface that significantly reduced the efficiency of

electron injection from the excited state of the dye molecule to the conduction band of TiO_2.[73] However, the *ortho*-substituted long alkoxyl chains in **119** exhibited dramatic effects to decrease the degree of dye aggregation so that the IPCE values of **119** were significantly improved by a factor of three over those of **121**. As a result, J_{SC} of the **119** device was improved by more than a factor of two over that of the **121** device. Therefore, the device performance of **119** reached efficiency of 6.03%, which was remarkably improved by 135% compared with that of **121** (Table 19).

Table 19. Photocatalytic parameters under global AM 1.5 irradiation for DSSCs absorbed on nanocrystalline TiO_2 anodes.

Dye	J_{sc}, mA cm^{-2}	V_{oc}, V	FF	n, %
105	11.30	0.696	0.737	5.80
106	7.17	0.673	0.755	3.64
118	15.37	0.745	0.702	8.04
119	11.59	0.720	0.723	6.03
120	14.6	0.713	0.721	7.23
121	5.09	0.679	0.743	2.57

3. PHOSPHONIC ACIDS AS ANCHORING GROUPS

Another group that has been used as an anchoring group is the phosphonic acid. An interesting study investigated the effects of the anchoring group (carboxylate *vs.* phosphonate) in ruthenium-bipyridyl-based complexes on the photoelectrochemical behaviors when they were used as sensitizers in DSSCs.[113] The surface binding on TiO_2 and the overall cell performance were highly dependent on both the number and the kind of anchoring groups. The cell performance (or sensitization efficiency) of carboxylate-TiO_2 systems was primarily governed by the surface binding mode and stability of carboxylate-complexes on TiO_2, which was strongly influenced by the number of the carboxylate groups. As a result, the tetra-carboxylateTiO_2 system showed the best cell performance despite the lowest visible light absorption because the most effective surface binding mode was allowed with this structure. On the contrary, the

photoelectrochemical behaviors of phosponate-TiO_2 systems were not influenced much by the surface binding properties. This could be attributed to the intrinsically stronger binding capability of the phosphonate group than the carboxylate linkage. Since the surface binding of phosphonate-complexes was strong enough even with only one phosphonate group, the presence of additional anchoring groups did not make a significant difference in the sensitizer adsorption and the electronic coupling between the sensitizer and TiO_2. Therefore, the overall cell performance followed the order of the visible light absorptivity of phosphonate-complexes, which changed with the number of phosphonate groups.

Phosphonic acid was placed at both *meso* and *β*- position of the porphyrin ring. For phosphonates there was evidence for both bi- and tridentate linkages, with bidentate theoretically determined to be the most stable on crystalline TiO_2 lattices (Figure 39).[114-118]

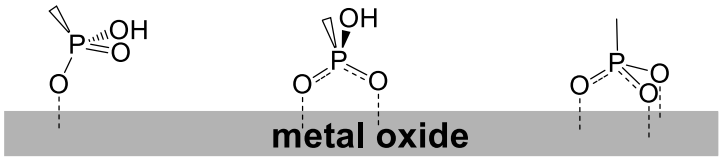

Figure 39. Different binding modes of phosphonates on TiO_2.

In an interesting study various porphyrins sensitizers were synthesized (Figure 40) and the type and the position of the anchoring group were studied.[43]

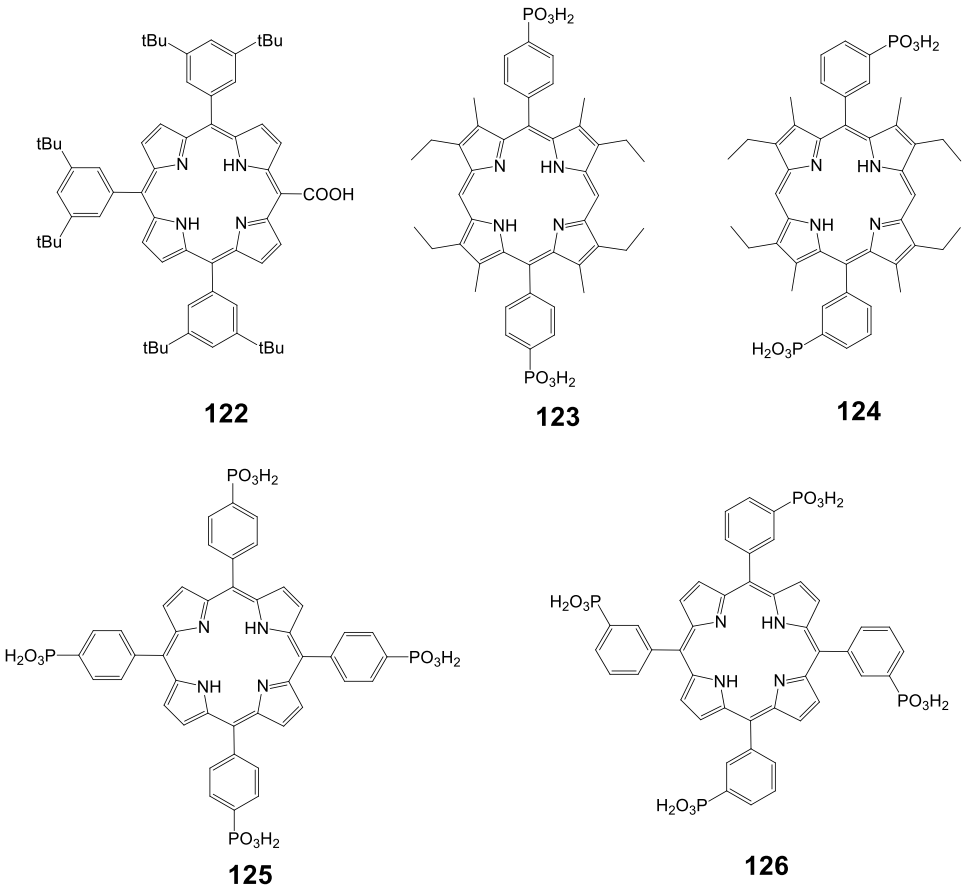

Figure 40. Molecular structure of dyes **122-126**.

In this study, it was shown that the nature of the anchoring group (phosphonic or carboxylic acids) had little impact on the photo-electrochemical performance of the cell. However, the substitution position of the anchoring group on the porphyrin strongly influenced the IPCE of the resulting cell. The results indicated that the electronic coupling of this type of dye with the *d*-band of the semiconductor was one of the key parameters in the design of efficient sensitizers.

Porphyrin **122** bears the COOH anchoring group directly on the *p*-aromatic core. This feature certainly allowed for a stronger electronic interaction with TiO_2 compared to porphyrin **1**, in which the remote COOH groups were electronically decoupled from the porphyrin macrocycle.

The sensitivity of the IPCE to the substitution position of the phosphonate anchoring groups in porphyrins **123** and **124** was also remarkable (Figure 40). This can be interpreted as due to differences in the orientation and distance of the dye with respect to the TiO_2 surface imposed by the directionality of the anchoring groups. The porphyrin that beard phosphonic acid groups in *meta* positions on the phenyl ring (dye

124) may lie closer to the TiO_2 surface than that with *para* substituents (dye **123**). Consequently, these variations may bring about significant differences in the magnitude of the electronic coupling. Activated electron transfer for dyes **124** and **125** can explain why the IPCE values of these sensitizers were the same and did not parallel the differences observed between dyes **123** and **124**. The injection quantum yield of the former sensitizers might be limited by the lower excited state potentials. Finally, it was noted that replacement of the phosphonic with the carboxylic functions, as in the case of **125** and **1**, did not seem to modify the dye photo-electrochemical performances. This could be explained by the fact that both dyes were electronically decoupled from TiO_2 because the *meso*-aryl groups orient perpendicularly to the porphyrin macrocycle.

In another study two porphyrins (**127** and **128**) were synthesized bearing a phosphonic acid at the *beta* position of the porphyrin ring (Figure 41) and were compared with the same porphyrins with carboxylic acid as anchoring groups.[46] It was reported that porphyrin **128** showed much lower efficiency (0.89 %) compared to the same porphyrin with a carboxylate anchoring group (4.11%), (Table 20).

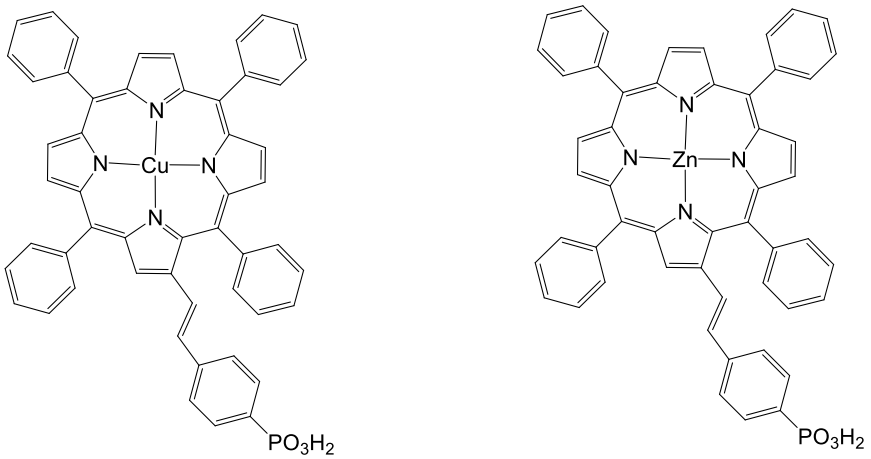

Figure 41. Molecular structure of dyes **127** and **128**.

Table 20. Photovolataic performances of DSSC using 1**27** and **128.**

Dye	J_{sc}, mA cm^{-2}	V_{oc}, mV	FF	*n*%
127	1.1	561	0.67	0.41

128	2.05	580	0.75	0.89

4. SULFONIC ACIDS AS ANCHORING GROUPS

A systematic study on the functional groups (including sulfonic acids) of porphyrin derivatives was carried out by various spectroscopic measurements to reveal the effects of these groups on the photochemical properties and conversion efficiency (Figure 42).[42] The adsorption behaviors of three kinds of porphyrins were different on the surface of the TiO_2 electrode. An interaction between the porphyrin and the TiO_2 surface was observed, and their strengths were quite different and decreased in the order **1** > **129** > **130**. The ionization potentials of the porphyrins in the bulk and adsorbed onto the TiO_2 electrode were determined, and a shift in the ionization potential between the two states was found. This approach provided a method to determine the energy level for a semiconductor sensitized by dye under the working conditions. The type of the functional groups on the dye significantly influenced the photocurrent and the conversion efficiency. These results indicated that the binding state between the dye and semiconductor was an important factor affecting the properties of the dye-sensitized solar cell.

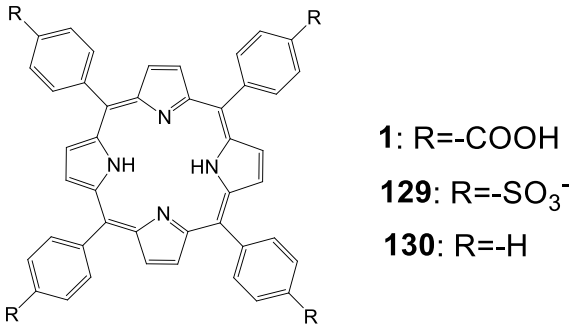

Figure 42. Molecular structure of dyes **1, 129** and **130**.

5. PYRIDINES AS ANCHORING GROUPS

A new type of push-pull dye sensitizer with a pyridine ring as an electron withdrawing anchoring group was developed.[119,120] These dyes exhibited a higher short circuit photocurrent (J_{sc}) and PCE compared to their counterpart dyes having carboxyl

groups. It was reported that the formation of coordinate bonds between the pyridine ring of the dye and the Lewis acid sites of the TiO_2 surface led to efficient electron injection owing to good electron communication between them rather than the formation of an ester linkage between the dyes having a carboxyl anchoring group.

Three porphyrin dyes, **131**, **132** and **133** (Figure 43), bearing one, two and four pyridyl groups, respectively, in the meso positions, acting as electron acceptor anchoring groups, were synthesized, characterized and investigated as sensitizers for the fabrication of DSSCs.[121] The overall PCEs of DSSCs based on these dyes laid in the range of 2.46–3.9% using a 12 mm thick TiO_2 photoanode. Porphyrin **132** achieved the maximum performance, which could be rationalized by the high dye loading, efficient electron injection, dye regeneration process and longer electron lifetime, as demonstrated by the electrochemical impedance spectroscopy (EIS) measurements (Table 21). The PCE of the DSSC of sensitizer **132** when the photoanode was treated with formic acid, showed an enhanced efficiency of 5.23% (J_{sc} = 12.04 mA/cm^2, V_{oc} = 0.68 V and FF = 0.64). This improvement, attributed to multifunctional properties such as higher dye uptake, reduced recombination process and enhanced charge collection efficiency.

Deoxycholic acid (DCA) was also used as a co-adsorbent in order to prevent dye aggregation and it was found that the PCE improved up to 6.12% (J_{sc} = 12.86 mA/cm^2, V_{oc} = 0.70 V and FF = 0.68) for sensitizer **132** on the modified TiO_2 photoanode, which could be attributed to further improvement in the electron injection efficiency and charge collection efficiency.

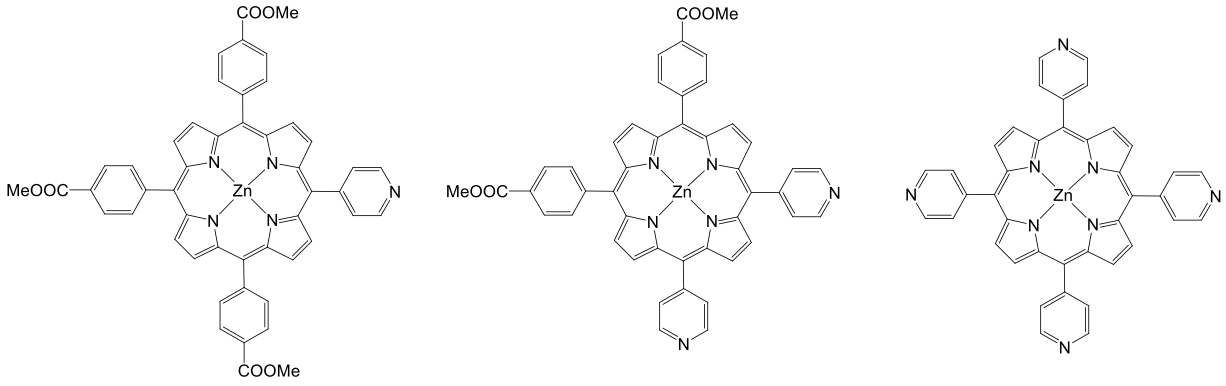

Figure 43. Molecular structure of dyes **131-133**.

Table 21. Photovolataic performances of DSSC using **131-133.**

Dye	J_{sc}, mA cm^{-2}	V_{oc}, V	FF	n%
131	9.2	0.60	0.56	3.10
132	10.56	0.64	0.60	3.90
133	7.6	0.60	0.54	2.46

A novel porphyrin dye extended at one *meso*-position *via* a pyridinylethynyl group acting as anchoring group and three phenyl COOMe groups was synthesized and used as sensitizer for the fabrication DSSC (Figure 44).[122] The overall PCE of DSSCs based on porphyrin **134** with and without chenodeoxychlolic acid (CDCA) as coadsorbant were 3.36% (J_{sc} = 9.38 mA/cm^2, V_{oc} = 0.64 V and FF = 0.56)and 4.56% (J_{sc} = 11.56 mA/cm^2, V_{oc} = 0.72 V and FF = 0.68), respectively. In order to improve the PCE of DSSC, Ag nanoparticles were incorporated into the nano-porous TiO_2 photoanode i.e. FTO/TiO_2/Ag-NPs and found an enhancement up to 5.66% (J_{sc} = 11.56 mA/cm^2, V_{oc} = 0.72 V and FF = 0.68). The improved photovoltaic performance of the DSSCs with modified photoanode was attributed to the (i) the increased light harvesting efficiency due to the plasmon enhanced optical absorption induced by Ag nanoparticles, (ii) reduced back recombination process at TiO_2/dye/electrolyte interface, (iii) improved electron lifetime, and (iv) formation of Schottky barrier at TiO_2/NPs-Ag.

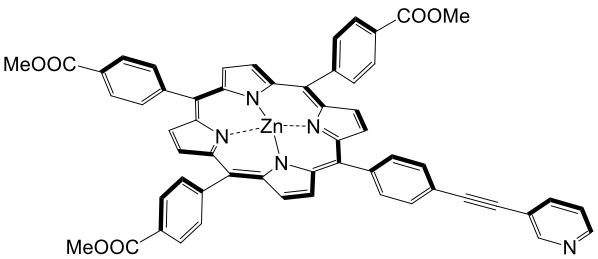

134

Figure 44. Molecular structure of dye **134**.

In another study,[123] it was investigated the effect of a thiourea containing electrolyte on the photovoltaic response of a DSSC based on an A_3B-type *meso* substituted porphyrin **134**. The porphyrin structure contained three methyl-benzoate and a phenylethynyl-pyridine group. The overall PCE of the DSSC based on thiourea containing electrolyte was 5.34% (J_{sc} = 11.93 mA/cm^2, V_{oc} = 0.70 V and FF = 0.64), which was higher than the corresponding DSSC without thiourea electrolyte (3.36%, J_{sc} = 9.38 mA/cm^2, V_{oc} = 0.64 V and FF = 0.56), under identical conditions.

Since the anchoring groups were extremely important in controlling the performance of dye-sensitized solar cells (DSSCs), the design of sensitizers with new anchoring groups became quite popular.[124] Therefore, donor-*p*-acceptor zinc-porphyrin dyes with a pyridine ring as an anchoring group designed and synthesized for DSSC applications (Figure 45). Photophysical and electrochemical investigations demonstrated that the pyridine ring worked effectively as an anchoring group for the porphyrin sensitizers. DSSCs that were based on these new porphyrins showed an overall power conversion efficiency of about 4.0% for compound **135** under full sunlight (AM 1.5G, 100 mWcm^2). Moreover, compounds **136**-**138** showed efficiencies of about 1, 4 and 9 %, respectively (Table 22).

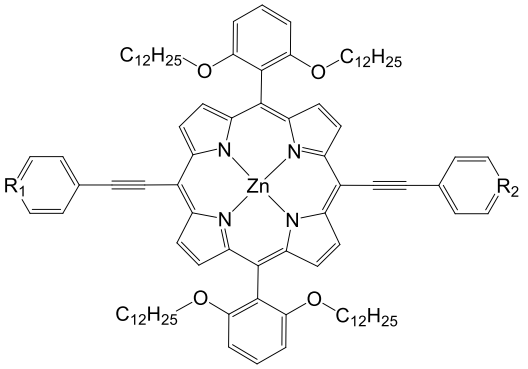

135: R_1=$CN(CH_3)_2$, R_2=N
136: R_1=N, R_2=N
137: R_1=CCOOH, R_2=CCOOH
138: R_1=$CN(CH_3)_2$, R_2=CCOOH

Figure 45. Molecular structure of dyes **135-138**.

Table 22. Photovolataic performances of DSSC using **135-138.**

Dye	J_{sc}, mA cm^{-2}	V_{oc}, V	FF	*n*%
135	8.2	0.63	0.77	3.96
136	2.84	0.54	0.74	1.24

137	9.83	0.63	0.74	4.59
138	17.38	0.73	0.71	9.01

6. CONCLUSIONS

In this review, we have covered porphyrin based systems for solar cells bearing various anchoring groups as an effective binding site onto TiO_2 electrode. The one that has been mostly used is the carboxylic acid, being *meso*-substituted or conjugated to the porphyrin ring at the *trans* or *β* position. Also, the most recent examples of phosphonic, sulfonic acids and pyridine anchoring groups are presented. The influence of various anchoring groups at the efficiency of the dyes is extensively discussed. In all the above examples, various donor groups have been added onto the porphyrinic macrocycle, with the diphenyl amide as a leading group. Since the best efficiency was present in a dye bearing a donor-acceptor group, much effort has been made towards this motif.

We strongly believe that the most promising approach is to develop panchromatic light harvesting single molecules that can absorb light over the entire visible/NIR spectrum and to achieve effective integration in photovoltaics. Innovative design strategies are necessary to avoid this problem. Along this path, a perfect combination of multiple sensitizers having complimentary absorption properties over the whole visible and NIR region (400–920 nm) is particularly promising. In addition, energy cascading by relay dyes exhibiting complimentary overlap between emission of one dye and absorption of another are also very interesting. Moreover, broad absorption by self-assembled or orderly aggregated dyes also poses encouraging aspects for photovoltaics if the side reactions or efficiency retarding interactions could be minimized inside the cell. Toward this aim, we believe that porphyrins offer an excellent platform for building such multi-chromophoric systems to self-assembly because the availability of several substituent sites and their intrinsic spectroscopic properties. Much deeper understanding of structural and functional features of natural light-harvesting systems is required for judicious design of more efficient single porphyrin molecules and multiporphyrin systems. Finally, appropriate physical

requirements and advanced strategies are needed to assimilate these developments into the device that can utilize and transform light into other forms of storable energy.

7. ACKNOWLEDGMENTS

Financial support from the European Commission (FP7-REGPOT-2008-1, Project BIOSOLENUTI No 229927) is greatly acknowledged. This research has been also co-financed by the European Union (European Social Fund–ESF) and Greek national funds through the Operational Program "Education and Lifelong Learning" of the National Strategic Reference Framework (NSRF)-Research Funding Program: Heraklitos II and THALIS-UOA-MIS 377252. Finally Special Research account of the University of Crete is also acknowledged.

8. REFERENCES

(1) W., C. G.; S., L. N. *Phys. Today* **2007**, *60*, 37.
(2) O'Regan, B.; Gratzel, M. *Nature* **1991**, *353*, 737.
(3) Nazeeruddin, M. K.; Kay, A.; Rodicio, I.; Humphry-Baker, R.; Mueller, E.; Liska, P.; Vlachopoulos, N.; Graetzel, M. *J. Am. Chem. Soc.* **1993**, *115*, 6382.
(4) Grätzel, M. *Acc. Chem. Res.* **2009**, *42*, 1788.
(5) Hagfeldt, A.; Boschloo, G.; Sun, L.; Kloo, L.; Pettersson, H. *Chem. Rev.* **2010**, *110*, 6595.
(6) Hardin, B. E.; Snaith, H. J.; McGehee, M. D. *Nat. Photon.* **2012**, *6*, 162.
(7) Giribabu, L.; Kanaparthi, R. K.; Velkannan, V. *Chem. Rec.* **2012**, *12*, 306.
(8) Nazeeruddin, M. K.; De Angelis, F.; Fantacci, S.; Selloni, A.; Viscardi, G.; Liska, P.; Ito, S.; Takeru, B.; Grätzel, M. *J. Am. Chem. Soc.* **2005**, *127*, 16835.
(9) Wang, Q.; Ito, S.; Grätzel, M.; Fabregat-Santiago, F.; Mora-Seró, I.; Bisquert, J.; Bessho, T.; Imai, H. *J. Phys. Chem. B* **2006**, *110*, 25210.
(10) Chen, C.-Y.; Wang, M.; Li, J.-Y.; Pootrakulchote, N.; Alibabaei, L.; Ngoc-le, C.-h.; Decoppet, J.-D.; Tsai, J.-H.; Grätzel, C.; Wu, C.-G.; Zakeeruddin, S. M.; Grätzel, M. *ACS Nano* **2009**, *3*, 3103.
(11) Cao, Y.; Bai, Y.; Yu, Q.; Cheng, Y.; Liu, S.; Shi, D.; Gao, F.; Wang, P. *J. Phys. Chem. C* **2009**, *113*, 6290.
(12) Yu, Q.; Wang, Y.; Yi, Z.; Zu, N.; Zhang, J.; Zhang, M.; Wang, P. *ACS Nano* **2010**, *4*, 6032.
(13) Han, L.; Islam, A.; Chen, H.; Malapaka, C.; Chiranjeevi, B.; Zhang, S.; Yang, X.; Yanagida, M. *Energ. Environ. Sci.* **2012**, *5*, 6057.
(14) Nazeeruddin, M. K.; Baranoff, E.; Grätzel, M. *Sol. Energy* **2011**, *85*, 1172.
(15) Campbell, W. M.; Burrell, A. K.; Officer, D. L.; Jolley, K. W. *Coord. Chem. Rev.* **2004**, *248*, 1363.

(16) Walter, M. G.; Rudine, A. B.; Wamser, C. C. *J. Porphyrins Phthalocyanines* **2010**, *14*, 759.
(17) Li, L. L.; Diau, E. W. G. *Chem. Soc. Rev.* **2013**, *42*, 291.
(18) Giribabu, L.; Kumar, C. V.; Reddy, P. Y. *J. Porphyrins Phthalocyanines* **2006**, *10*, 1007.
(19) Mandalia, H. C.; Jain, V. K.; Pattanaik, B. N. *J. Chem. Sci.* **2012**, *2*, 89.
(20) Giribabu, L.; Kanaparthi, R. K. *Curr. Sci.* **2013**, *104*, 847.
(21) Zeng, W.; Cao, Y.; Bai, Y.; Wang, Y.; Shi, Y.; Zhang, M.; Wang, F.; Pan, C.; Wang, P. *Chem. Mater.* **2010**, *22*, 1915.
(22) Deisenhofer, J.; Norris, J. R. *The Photosynthetic Reaction* Academic Press, New York, **1993**.
(23) Luo, L.; Lo, C.-F.; Lin, C.-Y.; Chang, I. J.; Diau, E. W.-G. *J. Phys. Chem. B* **2005**, *110*, 410.
(24) Lin, C.-Y.; Lo, C.-F.; Luo, L.; Lu, H.-P.; Hung, C.-S.; Diau, E. W.-G. *J. Phys. Chem. C* **2008**, *113*, 755.
(25) O'Regan, B. C.; López-Duarte, I.; Martínez-Díaz, M. V.; Forneli, A.; Albero, J.; Morandeira, A.; Palomares, E.; Torres, T.; Durrant, J. R. *J. Am. Chem. Soc.* **2008**, *130*, 2906.
(26) Cid, J.-J.; Yum, J.-H.; Jang, S.-R.; Nazeeruddin, M. K.; Martínez-Ferrero, E.; Palomares, E.; Ko, J.; Grätzel, M.; Torres, T. *Angew. Chem. Int. Ed.* **2007**, *46*, 8358.
(27) Imahori, H.; Umeyama, T.; Ito, S. *Acc. Chem. Res.* **2009**, *42*, 1809.
(28) Gouterman, M. *J. Mol. Spectrosc.* **1961**, *6*, 138.
(29) Hsieh, C.-P.; Lu, H.-P.; Chiu, C.-L.; Lee, C.-W.; Chuang, S.-H.; Mai, C.-L.; Yen, W.-N.; Hsu, S.-J.; Diau, E. W.-G.; Yeh, C.-Y. *J. Mater. Chem.* **2010**, *20*, 1127.
(30) Bessho, T.; Zakeeruddin, S. M.; Yeh, C.-Y.; Diau, E. W.-G.; Grätzel, M. *Angew. Chem. Int. Ed.* **2010**, *49*, 6646.
(31) He, H.; Gurung, A.; Si, L. *Chem. Commun.* **2012**, *48*, 5910.
(32) Zhou, W.; Cao, Z.; Jiang, S.; Huang, H.; Deng, L.; Liu, Y.; Shen, P.; Zhao, B.; Tan, S.; Zhang, X. *Org. Electron.* **2012**, *13*, 560.
(33) Kang, M. S.; Kang, S. H.; Kim, S. G.; Choi, I. T.; Ryu, J. H.; Ju, M. J.; Cho, D.; Lee, J. Y.; Kim, H. K. *Chem. Commun.* **2012**, *48*, 9349.
(34) Jiao, C.; Zu, N.; Huang, K.-W.; Wang, P.; Wu, J. *Org. Lett.* **2011**, *13*, 3652.
(35) Lee, C.-W.; Lu, H.-P.; Lan, C.-M.; Huang, Y.-L.; Liang, Y.-R.; Yen, W.-N.; Liu, Y.-C.; Lin, Y.-S.; Diau, E. W.-G.; Yeh, C.-Y. *Chem. -Eur. J.* **2009**, *15*, 1403.
(36) Yella, A.; Lee, H.-W.; Tsao, H. N.; Yi, C.; Chandiran, A. K.; Nazeeruddin, M. K.; Diau, E. W.-G.; Yeh, C.-Y.; Zakeeruddin, S. M.; Grätzel, M. *Science* **2011**, *334*, 629.
(37) Murakoshi, K.; Kano, G.; Wada, Y.; Yanagida, S.; Miyazaki, H.; Matsumoto, M.; Murasawa, S. *J. Electroanal. Chem.* **1995**, *396*, 27.
(38) Clifford, J. N.; Palomares, E.; Nazeeruddin, M. K.; Grätzel, M.; Nelson, J.; Li, X.; Long, N. J.; Durrant, J. R. *J. Am. Chem. Soc.* **2004**, *126*, 5225.
(39) Palomares, E.; Martinez-Diaz, M. V.; Haque, S. A.; Torres, T.; Durrant, J. R. *Chem. Commun.* **2004**, 2112.
(40) Durrant, J. R.; Haque, S. A.; Palomares, E. *Coord. Chem. Rev.* **2004**, *248*, 1247.
(41) Ma, T.; Inoue, K.; Yao, K.; Noma, H.; Shuji, T.; Abe, E.; Yu, J.; Wang, X.; Zhang, B. *J. Electroanal. Chem.* **2002**, *537*, 31.
(42) Ma, T.; Inoue, K.; Noma, H.; Yao, K.; Abe, E. *J. Photochem. Photobiol. A* **2002**, *152*, 207.
(43) Odobel, F.; Blart, E.; Lagree, M.; Villieras, M.; Boujtita, H.; El Murr, N.; Caramori, S.; Alberto Bignozzi, C. *J. Mater. Chem.* **2003**, *13*, 502.
(44) Wang, Q.; Campbell, W. M.; Bonfantani, E. E.; Jolley, K. W.; Officer, D. L.; Walsh, P. J.; Gordon, K.; Humphry-Baker, R.; Nazeeruddin, M. K.; Grätzel, M. *J. Phys. Chem. B* **2005**, *109*, 15397.
(45) Nazeeruddin, M. K.; Humphry-Baker, R.; Liska, P.; Grätzel, M. *J. Phys. Chem. B* **2003**, *107*, 8981.

(46) Nazeeruddin, M. K.; Humphry-Baker, R.; Officer, D. L.; Campbell, W. M.; Burrell, A. K.; Grätzel, M. *Langmuir* **2004**, *20*, 6514.

(47) Screen, T. E. O.; Lawton, K. B.; Wilson, G. S.; Dolney, N.; Ispasoiu, R.; Goodson Iii, T.; Martin, S. J.; Bradley, D. D. C.; Anderson, H. L. *J. Mater. Chem.* **2001**, *11*, 312.

(48) Lin, V. S.; DiMangno, S. G.; Therien, M. J. *Science* **1994**, *264*, 1105.

(49) Kalyanasundaram, K.; Vlachopoulos, N.; Krishnan, V.; Monnier, A.; Graetzel, M. *J. Phys. Chem.* **1987**, *91*, 2342.

(50) Kay, A.; Graetzel, M. *J. Phys. Chem.* **1993**, *97*, 6272.

(51) Cherian, S.; Wamser, C. C. *J. Phys. Chem. B* **2000**, *104*, 3624.

(52) Schmidt, E. S.; Calderwood, T. S.; Bruice, T. C. *Inorg. Chem.* **1986**, *25*, 3718.

(53) Seth, J.; Palaniappan, V.; Johnson, T. E.; Prathapan, S.; Lindsey, J. S.; Bocian, D. F. *J. Am. Chem. Soc.* **1994**, *116*, 10578.

(54) Bruckner, C.; Foss, P. C. D.; Sullivan, J. O.; Pelto, R.; Zeller, M.; Birge, R. R.; Crundwell, G. *Phys. Chem. Chem. Phys.* **2006**, *8*, 2402.

(55) Rochford, J.; Chu, D.; Hagfeldt, A.; Galoppini, E. *J. Am. Chem. Soc.* **2007**, *129*, 4655.

(56) Rangan, S.; Katalinic, S.; Thorpe, R.; Bartynski, R. A.; Rochford, J.; Galoppini, E. *J. Phys. Chem. C* **2009**, *114*, 1139.

(57) Rochford, J.; Galoppini, E. *Langmuir* **2008**, *24*, 5366.

(58) Deacon, G. B.; Phillips, R. J. *Coord. Chem. Rev.* **1980**, *33*, 227.

(59) Finnie, K. S.; Bartlett, J. R.; Woolfrey, J. L. *Langmuir* **1998**, *14*, 2744.

(60) Vittadini, A.; Selloni, A.; Rotzinger, F. P.; Grätzel, M. *J. Phys. Chem. B* **2000**, *104*, 1300.

(61) Imahori, H.; Hayashi, S.; Hayashi, H.; Oguro, A.; Eu, S.; Umeyama, T.; Matano, Y. *J. Phys. Chem. C* **2009**, *113*, 18406.

(62) Imahori, H.; Matsubara, Y.; Iijima, H.; Umeyama, T.; Matano, Y.; Ito, S.; Niemi, M.; Tkachenko, N. V.; Lemmetyinen, H. *J. Phys. Chem. C* **2010**, *114*, 10656.

(63) Park, J. K.; Chen, J.; Lee, H. R.; Park, S. W.; Shinokubo, H.; Osuka, A.; Kim, D. *J. Phys. Chem. C* **2009**, *113*, 21956.

(64) Mozer, A. J.; Griffith, M. J.; Tsekouras, G.; Wagner, P.; Wallace, G. G.; Mori, S.; Sunahara, K.; Miyashita, M.; Earles, J. C.; Gordon, K. C.; Du, L.; Katoh, R.; Furube, A.; Officer, D. L. *J. Am. Chem. Soc.* **2009**, *131*, 15621.

(65) Dy, J. T.; Tamaki, K.; Sanehira, Y.; Nakazaki, J.; Uchida, S.; Kubo, T.; Segawa, H. *Electrochemistry* **2009**, *77*, 206.

(66) Liu, Y.; Lin, H.; Dy, J. T.; Tamaki, K.; Nakazaki, J.; Nakayama, D.; Uchida, S.; Kubo, T.; Segawa, H. *Chem. Commun.* **2011**, *47*, 4010.

(67) Hart, A. S.; Kc, C. B.; Gobeze, H. B.; Sequeira, L. R.; D'Souza, F. *ACS Appl. Mater. Interfaces* **2013**, *5*, 5314.

(68) Zervaki, G. E.; Roy, M. S.; Panda, M. K.; Angaridis, P. A.; Chrissos, E.; Sharma, G. D.; Coutsolelos, A. G. *Inorg. Chem.* **2013**, *52*, 9813.

(69) Reddy, P. Y.; Giribabu, L.; Kumar, C. V. *J. Porphyrins Phthalocyanines* **2006**, *10*, 1007.

(70) Ambre, R. B.; Chang, G.-F.; Zanwar, M. R.; Yao, C.-F.; Diau, E. W.-G.; Hung, C.-H. *Chem. -Asian. J.* **2013**, *8*, 2144.

(71) Ambre, R. B.; Chang, G.-F.; Hung, C.-H. *Chem. Commun.* **2014**, *50*, 725.

(72) Stromberg, J. R.; Marton, A.; Kee, H. L.; Kirmaier, C.; Diers, J. R.; Muthiah, C.; Taniguchi, M.; Lindsey, J. S.; Bocian, D. F.; Meyer, G. J.; Holten, D. *J. Phys. Chem. C* **2007**, *111*, 15464.

(73) Lu, H.-P.; Mai, C.-L.; Tsia, C.-Y.; Hsu, S.-J.; Hsieh, C.-P.; Chiu, C.-L.; Yeh, C.-Y.; Diau, E. W.-G. *Phys. Chem. Chem. Phys.* **2009**, *11*, 10270.

(74) Lu, H.-P.; Tsai, C.-Y.; Yen, W.-N.; Hsieh, C.-P.; Lee, C.-W.; Yeh, C.-Y.; Diau, E. W.-G. *J. Phys. Chem. C* **2009**, *113*, 20990.

(75) Jensen, R. A.; Van Ryswyk, H.; She, C.; Szarko, J. M.; Chen, L. X.; Hupp, J. T. *Langmuir* **2009**, *26*, 1401.

(76) Chang, C.-W.; Luo, L.; Chou, C.-K.; Lo, C.-F.; Lin, C.-Y.; Hung, C.-S.; Lee, Y.-P.; Diau, E. W.-G. *J. Phys. Chem. C* **2009**, *113*, 11524.

(77) Lin, C.-Y.; Lo, C.-F.; Luo, L.; Lu, H.-P.; Hung, C.-S.; Diau, E. W.-G. *J. Phys. Chem. C* **2009**, *113*, 755.

(78) Lin, C.-Y.; Wang, Y.-C.; Hsu, S.-J.; Lo, C.-F.; Diau, E. W.-G. *J. Phys. Chem. C* **2010**, *114*, 687.

(79) Luo, L.; Lin, C.-J.; Tsai, C.-Y.; Wu, H.-P.; Li, L.-L.; Lo, C.-F.; Lin, C.-Y.; Diau, E. W.-G. *Phys. Chem. Chem. Phys.* **2010**, *12*, 1064.

(80) Liu, B.; Zhu, W.; Wang, Y.; Wu, W.; Li, X.; Chen, B.; Long, Y.-T.; Xie, Y. *J. Mater. Chem.* **2012**, *22*, 7434.

(81) Kurotobi, K.; Toude, Y.; Kawamoto, K.; Fujimori, Y.; Ito, S.; Chabera, P.; Sundström, V.; Imahori, H. *Chem. -Eur. J.* **2013**, *19*, 17075.

(82) Wu, C.-H.; Chen, M.-C.; Su, P.-C.; Kuo, H.-H.; Wang, C.-L.; Lu, C.-Y.; Tsai, C.-H.; Wu, C.-C.; Lin, C.-Y. *J. Mater. Chem. A* **2014**, *2*, 991.

(83) Campbell, W. M.; Jolley, K. W.; Wagner, P.; Wagner, K.; Walsh, P. J.; Gordon, K. C.; Schmidt-Mende, L.; Nazeeruddin, M. K.; Wang, Q.; Grätzel, M.; Officer, D. L. *J. Phys. Chem. C* **2007**, *111*, 11760.

(84) Allegrucci, A.; Lewcenko, N. A.; Mozer, A. J.; Dennany, L.; Wagner, P.; Officer, D. L.; Sunahara, K.; Mori, S.; Spiccia, L. *Energ. Environ. Sci.* **2009**, *2*, 1069.

(85) Armel, V.; Pringle, J. M.; Forsyth, M.; MacFarlane, D. R.; Officer, D. L.; Wagner, P. *Chem. Commun.* **2010**, *46*, 3146.

(86) Mozer, A. J.; Wagner, P.; Officer, D. L.; Wallace, G. G.; Campbell, W. M.; Miyashita, M.; Sunahara, K.; Mori, S. *Chem. Commun.* **2008**, 4741.

(87) Santos, T. D.; Morandeira, A.; Koops, S.; Mozer, A. J.; Tsekouras, G.; Dong, Y.; Wagner, P.; Wallace, G.; Earles, J. C.; Gordon, K. C.; Officer, D.; Durrant, J. R. *J. Phys. Chem. C* **2010**, *114*, 3276.

(88) Park, J. K.; Lee, H. R.; Chen, J.; Shinokubo, H.; Osuka, A.; Kim, D. *J. Phys. Chem. C* **2008**, *112*, 16691.

(89) Ishida, M.; Park, S. W.; Hwang, D.; Koo, Y. B.; Sessler, J. L.; Kim, D. Y.; Kim, D. *J. Phys. Chem. C* **2011**, *115*, 19343.

(90) Di, C. G.; Orbelli, B. A.; Pizzotti, M.; Tessore, F.; Trifiletti, V.; Ruffo, R.; Abbotto, A.; Amat, A.; De, A. F.; Mussini, P. R. *Chem. - Eur. J.* **2013**, *19*, 10723.

(91) Brennan, B. J.; Llansola Portoles, M. J.; Liddell, P. A.; Moore, T. A.; Moore, A. L.; Gust, D. *Phys. Chem. Chem. Phys.* **2013**, *15*, 16605.

(92) Balanay, M. P.; Kim, K. H.; Lee, S. H.; Kim, D. H. *J. Photochem. Photobiol., A* **2012**, *248*, 63.

(93) Liu, Y.; Xiang, N.; Feng, X.; Shen, P.; Zhou, W.; Weng, C.; Zhao, B.; Tan, S. *Chem. Commun.* **2009**, 2499.

(94) Nuay, V. A. K., Dong-Hee ; Lee, Sang-Hee ; Ko, Jae-Jung ; *Bull. Korean Chem. Soc.* **2009**, *2009*, 2871.

(95) Lee, C. Y.; Hupp, J. T. *Langmuir* **2009**, *26*, 3760.

(96) Lee, C. Y.; She, C.; Jeong, N. C.; Hupp, J. T. *Chem. Commun.* **2010**, *46*, 6090.

(97) Sirithip, K.; Morada, S.; Namuangruk, S.; Keawin, T.; Jungsuttiwong, S.; Sudyoadsuk, T.; Promarak, V. *Tetrahedron Lett.* **2013**, *54*, 2435.

(98) Griffith, M. J.; Sunahara, K.; Wagner, P.; Wagner, K.; Wallace, G. G.; Officer, D. L.; Furube, A.; Katoh, R.; Mori, S.; Mozer, A. J. *Chem. Commun.* **2012**, *48*, 4145.

(99) Lu, J.; Xu, X.; Cao, K.; Cui, J.; Zhang, Y.; Shen, Y.; Shi, X.; Liao, L.; Cheng, Y.; Wang, M. *J. Mater. Chem. A* **2013**, *1*, 10008.

(100) Kang, S. H.; Choi, I. T.; Kang, M. S.; Eom, Y. K.; Ju, M. J.; Hong, J. Y.; Kang, H. S.; Kim, H. K. *J. Mater. Chem. A* **2013**, *1*, 3977.

(101) Kang, M. S.; Choi, I. T.; Kim, Y. W.; You, B. S.; Kang, S. H.; Hong, J. Y.; Ju, M. J.; Kim, H. K. *J. Mater. Chem. A* **2013**, *1*, 9848.

(102) Reddy, N. M.; Pan, T. Y.; Rajan, Y. C.; Guo, B. C.; Lan, C. M.; Diau, E. W.; Yeh, C. Y. *Phys. Chem. Chem. Phys.* **2013**, *15*, 8409.

(103) Ripolles-Sanchis, T.; Guo, B. C.; Wu, H. P.; Pan, T. Y.; Lee, H. W.; Raga, S. R.; Fabregat-Santiago, F.; Bisquert, J.; Yeh, C. Y.; Diau, E. W. G. *Chem. Commun.* **2012**, *48*, 4368.

(104) Imahori, H.; Kang, S.; Hayashi, H.; Haruta, M.; Kurata, H.; Isoda, S.; Canton, S. E.; Infahsaeng, Y.; Kathiravan, A.; Pascher, T.; Chabera, P.; Yartsev, A. P.; Sundstrom, V. *J. Phys. Chem. A* **2011**, *115*, 3679.

(105) Eu, S.; Hayashi, S.; Umeyama, T.; Oguro, A.; Kawasaki, M.; Kadota, N.; Matano, Y.; Imahori, H. *J. Phys. Chem. C* **2007**, *111*, 3528.

(106) Eu, S.; Hayashi, S.; Umeyama, T.; Matano, Y.; Araki, Y.; Imahori, H. *J. Phys. Chem. C* **2008**, *112*, 4396.

(107) Tanaka, M.; Hayashi, S.; Eu, S.; Umeyama, T.; Matano, Y.; Imahori, H. *Chem. Commun.* **2007**, 2069.

(108) Hayashi, S.; Matsubara, Y.; Eu, S.; Hayashi, H.; Umeyama, T.; Matano, Y.; Imahori, H. *Chem. Lett.* **2008**, *37*, 846.

(109) Hayashi, S.; Tanaka, M.; Hayashi, H.; Eu, S.; Umeyama, T.; Matano, Y.; Araki, Y.; Imahori, H. *J. Phys. Chem. C* **2008**, *112*, 15576.

(110) Kira, A.; Matsubara, Y.; Iijima, H.; Umeyama, T.; Matano, Y.; Ito, S.; Niemi, M.; Tkachenko, N. V.; Lemmetyinen, H.; Imahori, H. *J. Phys. Chem. C* **2010**, *114*, 11293.

(111) Deshpande, R.; Wang, B.; Dai, L.; Jiang, L.; Hartley, C. S.; Zou, S.; Wang, H.; Kerr, L. *Chem. -Asian J.* **2012**, *7*, 2662.

(112) Hayashi, H.; Touchy, A. S.; Kinjo, Y.; Kurotobi, K.; Toude, Y.; Ito, S.; Saarenpaa, H.; Tkachenko, N. V.; Lemmetyinen, H.; Imahori, H. *ChemSusChem* **2013**, *6*, 508.

(113) Park, H.; Bae, E.; Lee, J.-J.; Park, J.; Choi, W. *J. Phys. Chem. B* **2006**, *110*, 8740.

(114) Bae, E.; Choi, W.; Park, J.; Shin, H. S.; Kim, S. B.; Lee, J. S. *J. Phys. Chem. B* **2004**, *108*, 14093.

(115) Rusu, C. N.; Yates, J. T. *J. Phys. Chem. B* **2000**, *104*, 12292.

(116) Luschtinetz, R.; Frenzel, J.; Milek, T.; Seifert, G. *J. Phys. Chem. C* **2009**, *113*, 5730.

(117) Guerrero, G.; Mutin, P. H.; Vioux, A. *Chem. Mater.* **2001**, *13*, 4367.

(118) Wang, P.; Klein, C.; Moser, J.-E.; Humphry-Baker, R.; Cevey-Ha, N.-L.; Charvet, R.; Comte, P.; Zakeeruddin, S. M.; Grätzel, M. *J. Phys. Chem. B* **2004**, *108*, 17553.

(119) Ooyama, Y.; Inoue, S.; Nagano, T.; Kushimoto, K.; Ohshita, J.; Imae, I.; Komaguchi, K.; Harima, Y. *Angew. Chem. Int. Ed.* **2011**, *50*, 7429.

(120) Ooyama, Y.; Nagano, T.; Inoue, S.; Imae, I.; Komaguchi, K.; Ohshita, J.; Harima, Y. *Chem. -Eur. J.* **2011**, *17*, 14837.

(121) Daphnomili, D.; Landrou, G.; Prakash Singh, S.; Thomas, A.; Yesudas, K.; K, B.; Sharma, G. D.; Coutsolelos, A. G. *RSC Adv.* **2012**, *2*, 12899.

(122) Daphnomili, D.; Sharma, G. D.; Biswas, S.; Justin, T. K. R.; Coutsolelos, A. G. *J. Photochem. Photobiol., A* **2013**, *253*, 88.

(123) Sharma, G. D.; Daphnomili, D.; Angaridis, P. A.; Biswas, S.; Coutsolelos, A. G. *Electrochim. Acta* **2013**, *102*, 459.

(124) Lu, J.; Xu, X.; Li, Z.; Cao, K.; Cui, J.; Zhang, Y.; Shen, Y.; Li, Y.; Zhu, J.; Dai, S.; Chen, W.; Cheng, Y.; Wang, M. *Chem. - Asian J.* **2013**, *8*, 956.